NASA/CR-1998-207471

IN-02-CR

FINAL REPORT: SUMMARY OF RESEARCH
GTRI PROJECT A-9483

CONTINUED DEVELOPMENT AND APPLICATION OF CIRCULATION CONTROL PNEUMATIC TECHNOLOGY TO ADVANCED TRANSPORT AIRCRAFT

NASA Grant NAG-1-1517

for:
NASA Langley Research Center
Subsonic Aerodynamics Branch, MS 286
Hampton, VA 23681-0001

by:
Robert J. Englar, Principal Research Engineer,
Principal Investigator

AEROSPACE AND TRANSPORTATION LABORATORY, CODE 0844
GEORGIA TECH RESEARCH INSTITUTE
GEORGIA INSTITUTE OF TECHNOLOGY
A Unit of the University System of Georgia
Atlanta, Georgia 30332-0844

Period Covered: June 14, 1993 to August 31, 1997

March 3, 1998

INTRODUCTION

Personnel of the Georgia Tech Research Institute (GTRI) Aerospace and Transportation Lab have completed a four-year grant program to develop and evaluate the pneumatic aerodynamic technology known as Circulation Control (CC) or Circulation Control Wing (CCW) for advanced transport aircraft. This pneumatic technology, which employs low-level blowing from tangential slots over round or near-round trailing edges of airfoils, greatly augments the circulation around a lifting or control surface and thus enhances the aerodynamic forces and moments generated by that surface. Two-dimensional force augmentations as high as 80 times the input blowing momentum coefficient have been recorded experimentally for these blown devices, thus providing returns of 8000% on the jet momentum expended. A further benefit is the absence of moving parts such as mechanical flaps, slats, spoilers, ailerons, elevators and rudders from these pneumatic surfaces, or the use of only very small, simple, blown aerodynamic surfaces on synergistic designs which integrate the lift, drag and control surfaces. The application of these devices to advanced aircraft can offer significant benefits in their performance, efficiency, simplicity, reliability, economic cost of operation, noise reduction, and safety of flight. To further develop and evaluate this potential, this research effort was conducted by GTRI under grant for the NASA Langley Research Center, Applied Aerodynamics Division, Subsonic Aerodynamics Branch, between June 14, 1993 and May 31, 1997. NASA personnel within this Branch which have served as Technical Monitors to GTRI during the conduct of this grant include, in chronological order:

Mr. Edgar G. Waggoner

Mr. Guy T. Kemmerly

Mr. Zachary T. Applin

Ms. Linda S. Bangert

GTRI personnel express our sincere thanks and appreciation for the assistance of these NASA personnel in the guidance and support of our research during this effort.

SUMMARY OF RESEARCH

Over these four years of experimental and computational-fluid-dynamic (CFD) development and evaluation, numerous pneumatic lift, control and stability concepts have been evaluated for low-speed operations of both subsonic and high-speed civil transports. Primary emphasis has been on high-lift, low-speed flight during takeoff and landing, as well as stable, controllable and safe flight under approach and climbout conditions. This effort includes development and evaluation of pneumatic airfoil and wing high-lift systems; leading-edge blowing and vortex-flap leading edges; pneumatic pitch, roll, and yaw devices; blown drag-control surfaces; and blown systems for control and safety of flight in regions of very high inflow directions (upwash, micro-bursts, down-drafts, etc.).

The results of these four years of grant research are summarized in the enclosed technical papers, which have been published in the general open literature. These include:

1. Englar, Robert J., Marilyn J. Smith, Sean M. Kelley and Richard C. Rover III, "**Application of Circulation Control Technology to Advanced Subsonic Transport Aircraft, Part I: Airfoil Development,**" AIAA Paper No. 93-0644; *AIAA Journal of Aircraft*, Vol. 31, No. 5, Sept.-Oct. 1994, pp. 1160-1168.

2. Englar, Robert J., Marilyn J. Smith, Sean M. Kelley and Richard C. Rover III, "**Application of Circulation Control Technology to Advanced Subsonic Transport Aircraft, Part II: Transport Application,**" AIAA Paper No. 93-0644; *AIAA Journal of Aircraft*, Vol. 31, No. 5, Sept.-Oct. 1994, pp. 1169-1177.

3. Englar, Robert J., "**Application of Pneumatic Lift and Control Surface Technology to Advanced Transport Aircraft,**" presented at *Transportation Beyond 2000: Engineering Design for the Future*, Conference at NASA Langley Research Center, Hampton, VA, September 26-28, 1995. Published in NASA Conference Proceedings, March 1996.

4. Englar, Robert J., Curt S. Niebur, and Scott D. Gregory, "**Pneumatic Lift and Control Surface Technology Applied to High Speed Civil Transport Configurations,** AIAA Paper No. 97-0036, presented at the AIAA 35th Aerospace Sciences Meeting and Exhibit, Reno, NV, January 6-10, 1997. Currently accepted for publication in the *AIAA Journal of Aircraft.*

As requested by both the NASA LaRC Grants Officer and the current NASA Technical Monitor to close out the existing grant, these published reports are thus submitted herein as the required Final Report and Summary of Research. It is anticipated that this pneumatic aerodynamic development effort will continue in the immediate future when NASA funds GTRI Proposal AERO 97 - 1047, "Additional Development and Systems Analyses of Pneumatic Technology for High-Speed Civil Transport Aircraft", which was submitted in April, 1997.

In accordance with NASA requirements, we hereby declare that no inventions have been made or filed by GTRI in relation to the work performed under this grant.

JOURNAL OF AIRCRAFT
Vol. 31, No. 5, Sept.–Oct. 1994

Application of Circulation Control to Advanced Subsonic Transport Aircraft, Part I: Airfoil Development

Robert J. Englar,* Marilyn J. Smith,† Sean M. Kelley,‡ and Richard C. Rover III‡
Georgia Tech Research Institute, Atlanta, Georgia 30332

An experimental/analytical research program was undertaken to develop advanced versions of circulation control wing (CCW) blown high-lift airfoils, and to address specific issues related to their application to subsonic transport aircraft. The primary goal was to determine the feasibility and potential of these pneumatic airfoils to increase high-lift system performance in the terminal area while reducing system complexity. A four-phase program was completed, including 1) experimental development and evaluation of advanced CCW high-lift configurations, 2) development of effective pneumatic leading-edge devices, 3) computational evaluation of CCW airfoil designs plus high-lift and cruise capabilities, and 4) investigation of the terminal-area performance of transport aircraft employing these airfoils. The first three phases of this program are described in Part I of this article. Applications to the high-lift and control systems of advanced subsonic transport aircraft and resulting performance are discussed in the continuation of this article, Part II. Experimental lift coefficient values approaching 8.0 at zero incidence and low blowing rates were demonstrated by two-dimensional CCW configurations that promised minimal degradation of the airfoil's performance during cruise. These results and experimental/CFD methods will be presented in greater detail in the following discussions.

Nomenclature

C_d = airfoil drag coefficient
C_l = airfoil lift coefficient
C_μ = two-dimensional jet momentum (blowing) coefficient, trailing-edge slot
$C_{\mu LE}$ = two-dimensional jet momentum (blowing) coefficient, leading-edge slot
c = airfoil chord length
c_f = flap chord length
h = blowing slot height, trailing edge
h_{LE} = blowing slot height, leading edge
$\dot{m}$ = jet mass flow rate per unit slot span
q = freestream dynamic pressure
r_1 = CCW flap radius of rotation
r_2 = CCW flap upper-surface radius
V_j = isentropic jet velocity
x_{slot} = longitudinal location of blowing slot
α = angle of attack
δ_f = flap deflection angle

Introduction

BASED on existing data,[1] pneumatic high-lift airfoils appear to offer significant payoffs in the design and development of next-generation subsonic transport aircraft. Both ground and flight experimental investigations have shown that a specific type of blown airfoil known as the circulation control wing (CCW) can greatly augment the high-lift capabilities of conventional mechanical flaps. Reference 1 provides summaries of some of these developments and includes verification of CCW airfoil sections generating very high lift at low blowing rates. It also discusses successful CCW applications to and flight tests on fixed-wing short takeoff and landing (STOL) and rotary-wing vertical takeoff and landing (VTOL) aircraft. The CCW concept employs tangential blowing over round or near-round trailing edges, as demonstrated on the airfoil seen in Fig. 1. Here, the lack of a sharp trailing edge avoids the Kutta condition requirement that the stagnation streamline depart the airfoil at the trailing edge. As can be seen in numerous experimental results,[2-5] the blowing jet causes the aft stagnation point to move nearly 180 deg around the round trailing edge. This action does, in fact, produce a pneumatic cambering device. The result is very high-lift generation, with two-dimensional lift coefficients greater than 7.0 being generated at 0-deg angle of attack.[2] Lift augmentation ($\Delta C_l/C_\mu$) as high as 80 or more has been reported in Refs. 1 and 6. The driving parameter is the momentum coefficient, defined for two-dimensional airfoils as

$$C_\mu = \dot{m}V_j/qc$$

Conversely, as Fig. 2 shows, a desired large lift increment due to blowing can be generated either at much lower blowing requirements than a conventional blown flap, or with a much smaller trailing-edge flap size.

In addition, high-lift system complexity can be reduced by substituting simplified pneumatic components for mechanical flaps, tracks, and actuators. Figure 1 shows a no-moving-parts CCW trailing edge applied to a NASA supercritical airfoil section.[7,8] Not only are the conventional leading-edge and trailing-edge components eliminated, but the resulting lift values (at zero incidence and up through maximum C_l) are quite significant. As this figure shows, CCW configurations applicable to transports typically generated C_l values up to 6 or 7, equal to or exceeding the high-lift potential of even the most complex multielement mechanical flap airfoils. In this case, the very large leading-edge radius of the thick blown airfoil produced attached flow up through 10-deg incidence, but it is obvious that more effective separation prevention was needed at higher incidence or higher lift. Pneumatic concepts can further simplify transport aircraft wings by eliminating the need for mechanical leading-edge devices as well as mechanical-roll-control or direct-lift-control surfaces.[9]

While the high-lift and simplifying capabilities of these CCW devices have been confirmed in experimental programs and in actual flight demonstrations on military aircraft,[10,11] specific

Presented as Paper 93-0644 at the AIAA 31st Aerospace Sciences Meeting and Exhibit, Reno, NV, Jan. 11–14, 1993; received April 27, 1993; revision received Feb. 25, 1994; accepted for publication March 7, 1994.

*Senior Research Engineer, Aerospace Sciences Laboratory. Associate Fellow AIAA.
†Senior Research Engineer, Aerospace Sciences Laboratory. Senior Member AIAA.
‡Cooperative Student, Aerospace Sciences Laboratory.

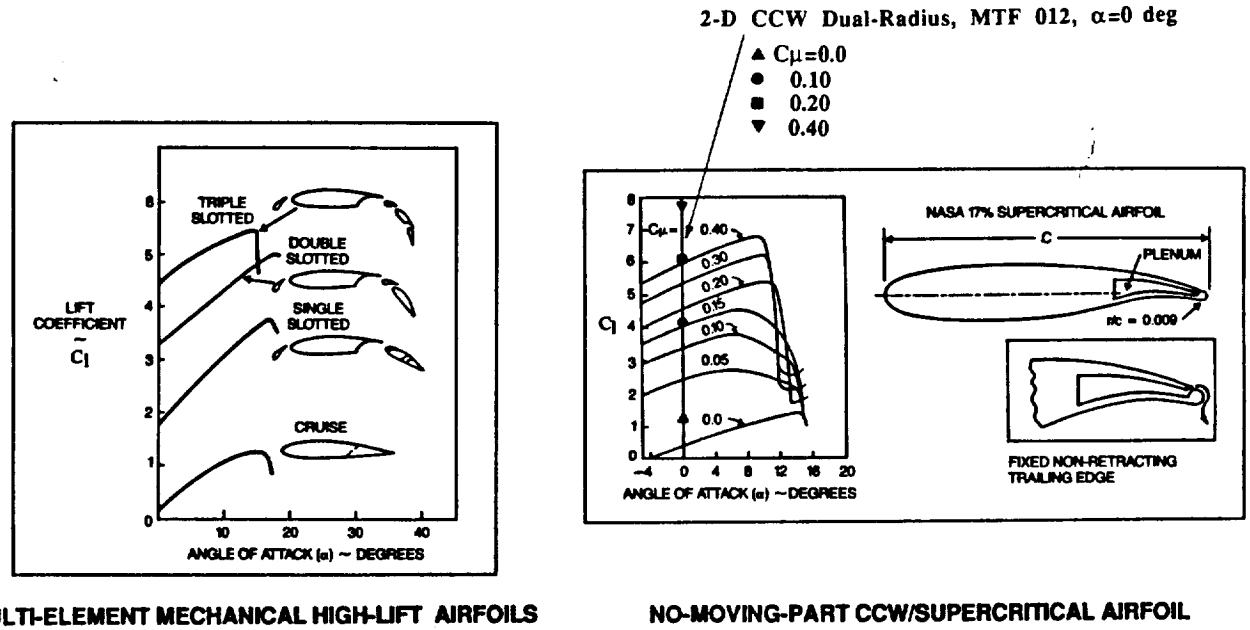

Fig. 1 Comparison of blown CCW and mechanical high-lift systems.

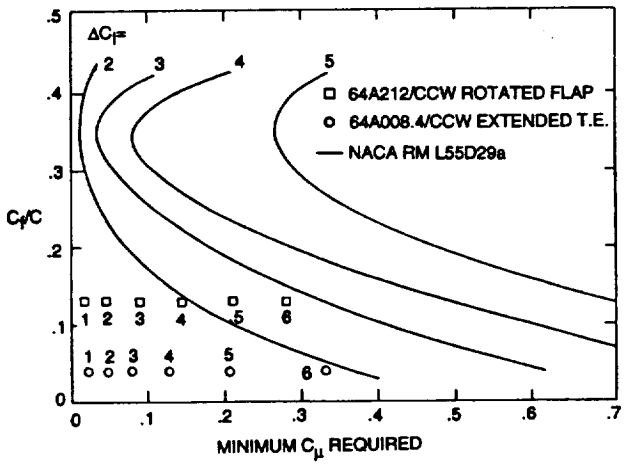

Fig. 2 Comparison of the lift-augmenting capabilities of blown flap and CCW airfoils at α = 0 deg.

application-related issues need to be addressed to take advantage of these pneumatic benefits for transport aircraft. Research personnel at the Aerospace Sciences Laboratory of Georgia Tech Research Institute (GTRI) have been involved with experimental development and computational analysis of these circulation control concepts since their initiation in the late 1960s. The present research project was undertaken by GTRI to resolve these issues in order to make pneumatic airfoil technology available for use in next-generation transports or as retrofits on existing aircraft. Specific issues to be addressed include the development of advanced CCW airfoils while minimizing airflow and blowing requirements; determining the feasibility and efficiency of pneumatic leading-edge devices; employing CFD computational methods to guide the design of CCW systems; and finally, investigating system performance for a postulated CCW subsonic transport (see Part II of this article). Results of the two-dimensional airfoil investigations will be presented in the following sections.

Development of Advanced CCW Airfoils

Prior CCW Configurations

Previous development of CCW high-lift airfoils has yielded a number of configurations intended for both fixed-wing STOL and rotary-wing VTOL aircraft; many of these have generated high-lift augmentation at low blowing rates. Whereas this lift augmentation is significant, the drag associated with large unblown radii can be prohibitive in cruise. An attempt to reduce that drag penalty was successful,[7,8] as much smaller trailing-edge radii were incorporated into the patented bluff trailing-edge configuration on a 17% supercritical airfoil (Fig. 1). While the drag was greatly reduced, it was found that small CCW radii with larger slot heights could cause jet detachment and sudden lift loss at higher C_μ. As a compromise to the above, the dual-radius CCW configuration was developed.[8] Figure 3 shows a typical CCW configuration of this type applied to a 16% thick supercritical airfoil. This configuration improves upon the round bluff CCW in three ways. First, the short-chord flap has a sharp trailing edge in the retracted configuration, so that in cruise there is very little increase in base drag or separated flow caused by the unblown round surface. Secondly, when this short flap is deflected about an initial radius r_1, the upper surface of the flap is a uniform circular arc with larger radius r_2. This is much more conducive to increased jet turning. Thirdly, the simple mechanical deflection also provides unblown camber, which adds to the total lift capability and provides some aerodynamic lift should a blowing loss occur. These advantages offer significant gains over the fixed round CCW configurations, even at the risk of adding some mechanical complexity. Thus, the development of advanced CCW configurations under the current effort has concentrated on the evaluation of these dual-radius configurations.

Two-Dimensional Airfoil Experimental Test Setup

Accurate two-dimensional experimental evaluation of blown high-lift airfoils is not a trivial undertaking, and considerable care must be expended to perform this effort properly.[12] The primary problem that must be overcome is the interaction between the momentum deficits in the tunnel-wall boundary layers and the severe adverse pressure gradients on the blown airfoil downstream of both the leading-edge and trailing-edge flaps or blowing slots. If left uncorrected, this yields strong vorticity at these junctions and nonuniform downwash all along the airfoil span; non-two-dimensional results are guaranteed, and the true angle of attack is far less than the nominal geometric value. For the present investigations conducted in the GTRI Model Test Facility (MTF) 30- × 43-in. subsonic research tunnel, a tangential wall blowing system previously developed at GTRI to improve ground-effect investigations[13] was modified to provide combined floor and ceiling blowing

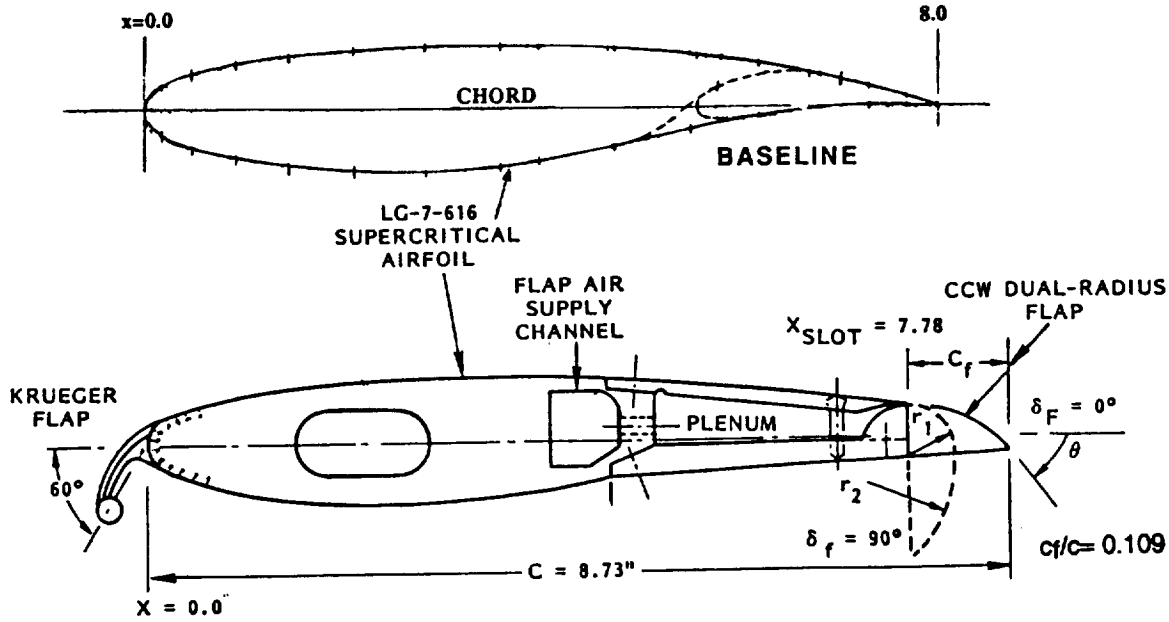

Fig. 3 Advanced dual-radius CCW configuration applied to a 16% thick supercritical two-dimensional airfoil model.

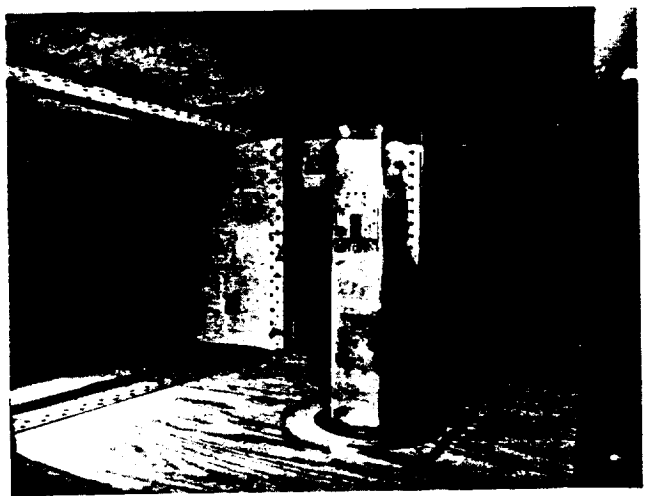

Fig. 4 Baseline two-dimensional CCW dual-radius airfoil in MTF test section, showing floor and ceiling wall blowing slots in entrance.

(Fig. 4). When applied to the present vertically-mounted airfoil tests, the calibrated wall blowing value that removed the wall interference also reduced the measured drag by up to 45% for the blown airfoils. This resulted from elimination of the induced drag due to vorticity at the walls. Static pressures measured along the model span also confirmed this blowing value as returning the spanwise flow to a near-uniform value from floor to ceiling. In addition to these spanwise pressures, chordwise static pressure measurements were taken on the model surface at midspan for comparison to CFD analytical results. Force and moment coefficients were recorded by a floor balance. The CCW model spanned almost 30 in. from tunnel floor to within $\frac{1}{8}$ in. of the tunnel ceiling, and was mounted on a 12-in.-diam base plate attached to the floor balance system. A thin endplate separated the ceiling end of the model from the wall, allowing only enough space to prevent model grounding. After the calibration of the ceiling blowing system, drag tares were taken on the base plate with wall blowing activated, and a blown tare as a function of dynamic pressure was determined. This increment was subtracted from all floor-balance data. Further explanation of test techniques, including mass flow/jet velocity tradeoffs (i.e., slot height vs pressure ratio), are given in Refs. 2, 4, 7, 8, and 12.

The airfoil of Fig. 3 was evaluated in this facility using these special two-dimensional test techniques. This configuration had previously been evaluated in the MTF tunnel as part of a powered-lift STOL program.[14] Those tests were conducted using a semi-span three-dimensional model with a constant-chord wing having this same airfoil section, and extending 26 in. from the tunnel floor, yielding an aspect-ratio-5.5 configuration. These semispan tests provided a good basis for evaluating the parameters of flap deflection, momentum coefficient, slot height and CCW turning radius, but their strong three dimensionality made them incompatible with previous high-quality two-dimensional data for other blown and mechanical-flap airfoils. Therefore, a rigorous effort was undertaken as part of the present program to accurately re-evaluate this baseline CCW dual-radius configuration as a two-dimensional airfoil. Although an improved version of this airfoil was designed using in-house CFD codes, the model conversion was not completed in time. Thus, the original dual-radius CCW/supercritical configuration of Fig. 3 was reinstalled in the GTRI Model Test Facility tunnel as a baseline reference two-dimensional airfoil model, Fig. 4.

Two-Dimensional Evaluation of Dual-Radius CCW Airfoil

Initially, force and moment coefficients plus static pressure distributions were recorded for this baseline CCW/Supercritical airfoil with the Krueger leading-edge flap deflected 60 deg and the 10.9% chord dual-radius flap deflected 90 deg. Figure 5 shows an aft view of the deflected flap with blowing applied. A cotton tuft reveals the large jet turning angle at the flap trailing edge. Figures 6 and 7 show reduced and corrected[12] balance data for this two-dimensional airfoil (labeled "MTF12") in comparison to data previously recorded for the semispan version of the same configuration (labeled "T158"), all taken at a geometric incidence of $\alpha = 0$ deg. The production data was taken at a dynamic pressure of 10 psf to limit larger aerodynamic loads and possible grounding of the balance, and is thus somewhat conservative, not taking advantage of the favorable Reynolds number effect shown. Also evaluated were the effects of variation in blowing slot height h (also discussed in Refs. 2, 4, 5, 7, and 8). In Fig. 6, two-dimensional lift values 26 to 43% greater than those of the semispan model are seen, primarily due to the elimination of the strong tip vorticity and improved test setup for the present two-dimensional data. Corresponding to this elimination of the induced finite-span effects are the 21–68% lower values of measured two-dimensional drag coefficient seen in

Fig. 5 Aft view of CCW dual-radius two-dimensional airfoil showing jet turning and attachment to 90-deg CCW flap.

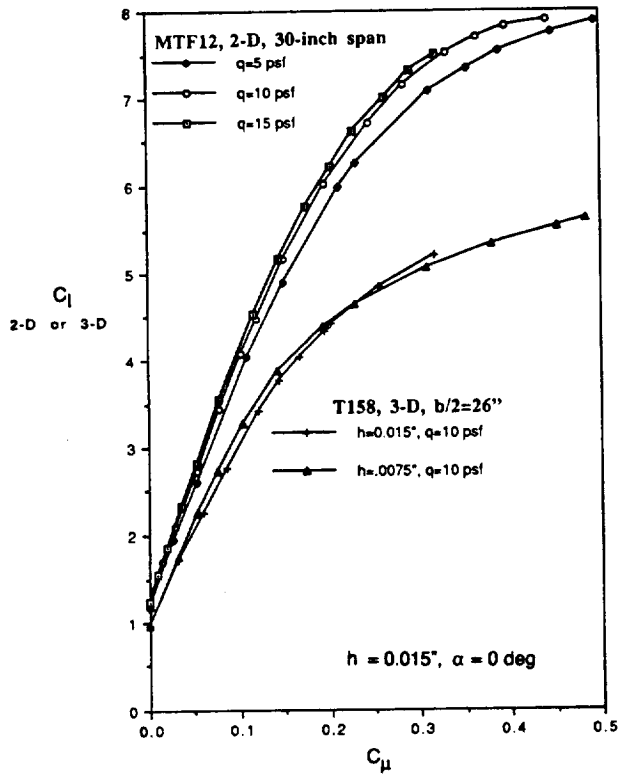

Fig. 6 Comparison of two-dimensional airfoil and three-dimensional semispan lift results for the dual-radius CCW model at $\alpha = 0$ deg (60-deg Krueger and 90-deg CCW flap deflections).

Fig. 7. These data emphasize the large difference between two- and three-dimensional data, and stress the importance of adequate two-dimensional test techniques.[12] Also of interest in Fig. 7 is the initial reduction of the two-dimensional drag as the blowing reduces separation on the highly deflected flap.

The above results represent a significant increase in lift-augmenting capability compared to previous CCW configu-

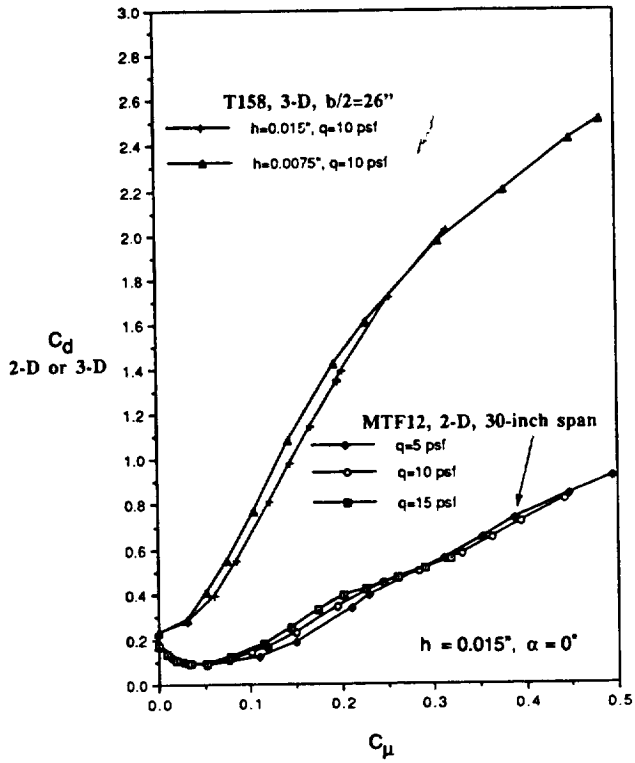

Fig. 7 Comparison of two-dimensional airfoil and three-dimensional semispan drag results for the dual-radius CCW model at $\alpha = 0$ deg (60-deg Krueger and 90-deg CCW flap deflections).

rations. In Fig. 1, the lift of this dual-radius CCW airfoil is compared at $\alpha = 0$ deg to the state-of-the-art high-lift airfoils and to earlier CCW configurations. Lift improvement of up to 35% over previous two-dimensional CCW airfoils is due partly to the increased unblown camber of the short-chord flap, and partly to the increased lift-augmentation capabilities provided by the greater CCW turning-surface radius on the flap. Lift values approaching 8.0 at 0-deg incidence and relatively low momentum coefficient represent a factor of from 1.8 to 4 increase over the zero-incidence lift values for the various mechanical flaps surveyed in Fig. 1. Furthermore, when these are added to a lift curve slope of 0.1/deg (or more, to be shown below), an effective leading-edge device should be able to yield $C_{l\,max}$ values in the 9 or greater range. It is significant to note that these two-dimensional pneumatic high-lift values recorded on the present CCW model are the highest ever recorded at these lower blowing rates by the first author in his 20+ yr of experience in test and evaluation of blown airfoils and wings.

This lift-generating ability is further emphasized by the static pressure distributions shown in Fig. 8, where very high trailing-edge suction peaks result in flow entrainment and circulation enhancement. However, even at $\alpha = 0$ deg, these distributions reveal the beginning of leading-edge separation on the Krueger flap at higher blowing, amplifying the need for a more effective pneumatic nonmechanical leading edge. Figure 9 shows variations in static pressure distributions as angle of attack is increased at a constant blowing value, and reveals the same type of LE separation.

To provide a baseline reference for the performance increase due to blowing on the dual-radius CCW, the flap was retracted to the cruise position (trailing edge located on the chord line), and the Krueger leading edge was removed. Figure 10 denotes the large aerodynamic differences between the high-lift and cruise configurations at 3 blowing rates: 0.0, 0.15, and 0.28. It also shows the increase in stall angle provided by the mechanical LE device. The augmentation effects of large jet turning, flow entrainment, and supercirculation on the overall airfoil characteristics are obvious. The dual-radius CCW

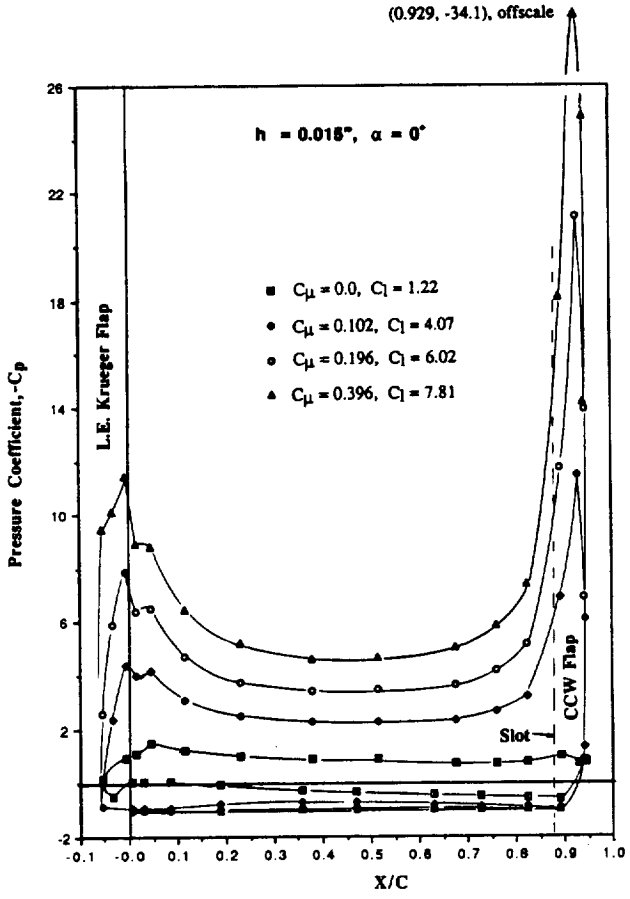

Fig. 8 Chordwise static pressure distributions for two-dimensional dual-radius CCW airfoil at $\alpha = 0$ deg and $q = 10$ psf (60-deg Krueger and 90-deg CCW flap deflections).

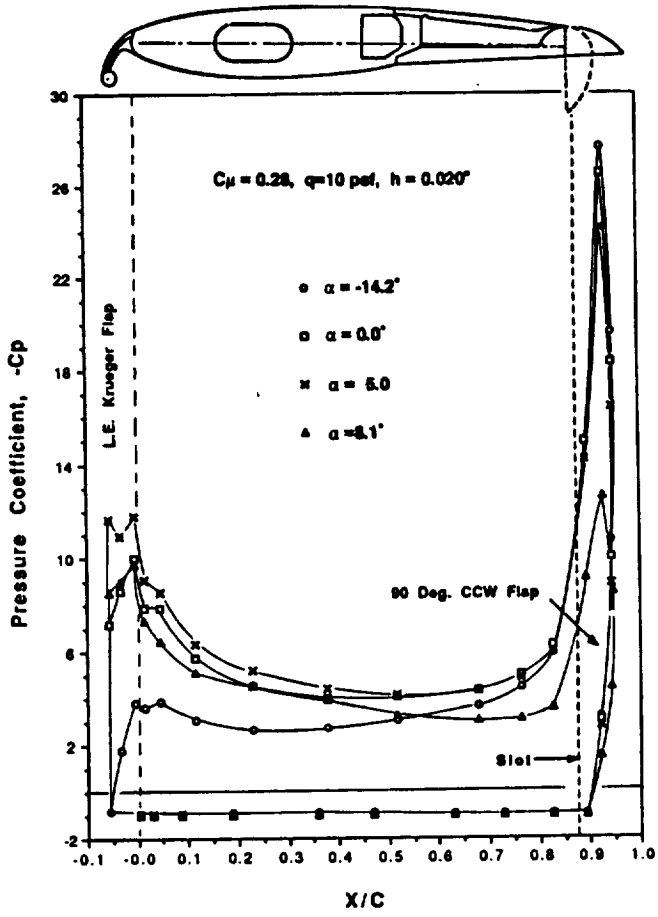

Fig. 9 Chordwise static pressure distributions for the dual-radius CCW airfoil, (60-deg Krueger and 90-deg CCW flap).

configuration with large deflections of the short-chord flap thus demonstrates very effective lift-generating capability as long as adequate leading-edge separation prevention is provided.

Pneumatic Leading-Edge Devices

Leading-Edge Effectiveness

Development of pneumatic or mechanical flap systems brings with it the essential requirement for effective leading-edge (LE) devices to prevent flow separation at large values of supercirculation, whether these values be produced by high incidence, mechanical camber, or pneumatic flow entrainment.[15] The current two-dimensional airfoil employs a Krueger leading-edge flap deflected 60 deg (Fig. 3), a state-of-the-art device commonly used on commercial and military transport aircraft. Its effectiveness in increasing stall angles and maximum lift coefficients is emphasized in Fig. 11, when compared to the same 90-deg-flap CCW airfoil with the Krueger flap retracted. The stall angle is increased by 6–7 deg for the unblown flap, and by 15 deg or more as flap C_μ is increased. However, the Krueger's effectiveness at high supercirculation values is still limited, as stall occurs at less than $\alpha = 5$ deg at higher C_μ values. Also, at lower lift and incidence, the 60-deg Krueger flap stalled on its lower surface. These results clearly emphasize the need for a more effective leading-edge device. To develop an appropriate blown leading edge, CFD codes (to be discussed below) were used to analyze suction peaks experienced in the leading-edge pressure distributions. Over an anticipated range of lift, blowing, and incidence, the blowing slot needed to be located slightly ahead of the adverse pressure gradient so that it could entrain the flowfield and delay separation.

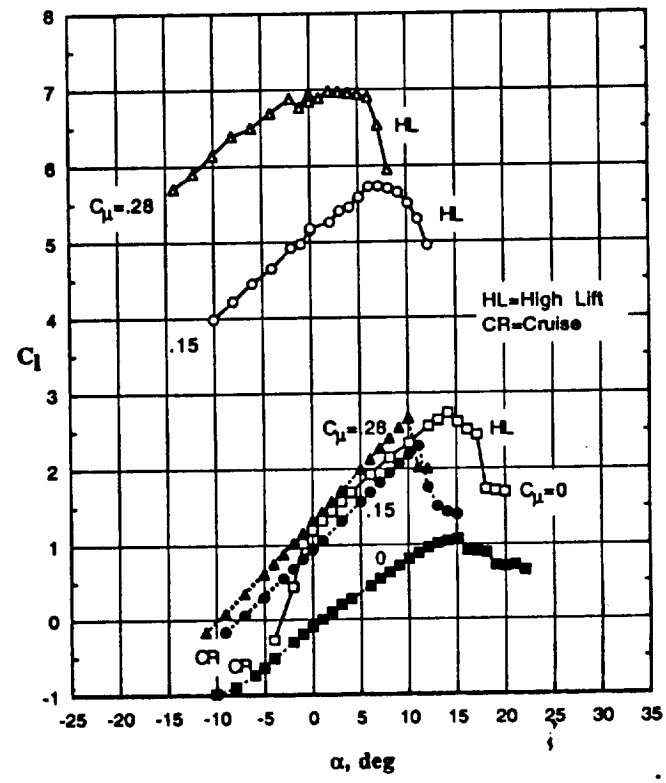

Fig. 10 Comparison of high-lift (60-deg Krueger and 90-deg CCW) and cruise CCW airfoil configurations.

Investigation of Dual-Slot CCW Airfoil

A preliminary dual-slot CCW airfoil was assembled by combining a CFD-designed blown leading-edge contour with the baseline CCW dual-radius aft flap assembly of Fig. 3. Figure 12 shows this model and the associated static pressure tap locations. Several slot height values and internal plenums were tested. The ability of this pneumatic LE to deter flow separation is shown in Fig. 13. Here, for two values of blowing on the CCW flap, variation in leading-edge blowing is shown. For reference, the clean (Krueger-retracted K_0) configuration is also shown. Compared to the clean leading edge, an increase of 2–4 deg in stall angle was produced by the aft-facing LE slot with blowing off. A significant gain in stall angle (10–13 deg) was produced by applying $C_{\mu LE} = 0.10$. Additional LE blowing above this amount was somewhat less productive. It was also found that increased LE blowing momentum was recovered as thrust (negative drag).

Figure 14 compares the effectiveness of LE blowing ($C_{\mu LE} = 0.18$) to the 60-deg Krueger flap. For zero and low CCW flap blowing, LE blowing has several strong effects. It extends the stall angle 6–7 deg beyond the Krueger value, eliminates the lower surface stall on the Krueger, and adds a lift increment while preserving the lift-curve slope. At higher CCW flap blowing, the pneumatic LE continues to yield higher stall angles than the Krueger, and makes the stall less severe by forcing aft rather than leading-edge separation. For all values of trailing-edge blowing, the Krueger LE is surpassed by the blown LE in both $C_{L\,max}$ and stall angle achieved. This improved LE performance was produced by a redesigned internal plenum yielding more uniform spanwise flow than from the original slot configuration. The known improvement[7,8,10] due to smaller slot height has been incorporated into this configuration. The uppermost curve of Fig. 14 shows the improvement in $C_{L\,max}$ and stall angle available if increased LE and TE blowing are available. The effectiveness of the pneumatic leading-edge has thus been verified as a means to extend the stall angle, increase usable lift and "soften" the stall.

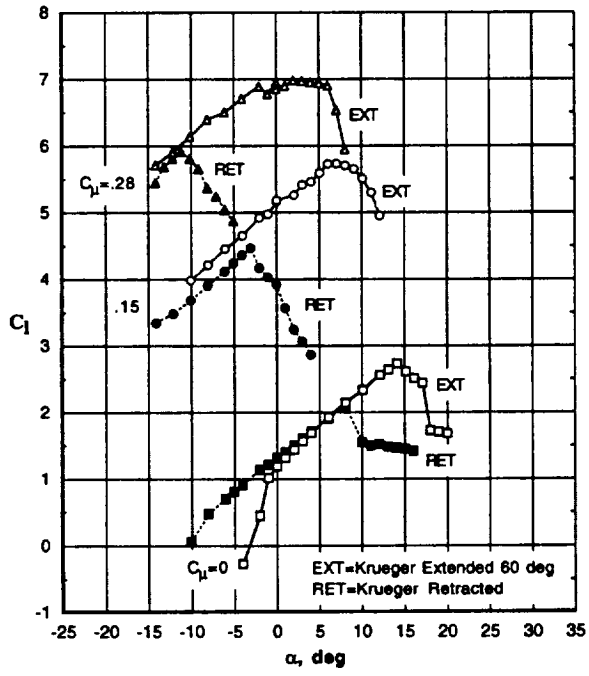

Fig. 11 Effect of adding Krueger leading-edge device to dual-radius airfoil with 90-deg CCW flap deflection.

This was further confirmed by the static pressure distributions shown in Figs. 9 and 15. Note the significant differences in the vicinity of the leading edge. The high LE jet velocity yields high negative pressure coefficients (Fig. 15) compared to those of the Krueger flap (Fig. 9). The concept of a blown leading edge offers significant potential here. The mechanical retraction/deployment components are eliminated. When blowing is terminated, the device becomes transparent. It does not experience lower surface stall at low incidence, and it surpasses the Krueger flap in keeping leading-edge flow attached at high incidence and lift. In addition, if applied in conjunction with a blown trailing-edge flap, its blowing schedule can be coupled directly to that of the flap, so that increased leading-edge protection occurs with increased supercirculation. The experimental evaluations thus confirmed these high-lift capabilities of CCW airfoils, and that this lift could be augmented by variations in angle of attack, blowing coefficients, flap deflections, and/or blowing slot heights.

Analytical Development of Circulation Control Airfoils

Design of the improved CCW airfoils was aided by the use of in-house viscous-flow CFD codes. The complex flowfields about circulation control (CC) airfoils with multiple jets are governed by highly interactive viscous and inviscid flow regions. Previous lower-order methods for computational analysis of single-slot CC airfoils[16–19] have consisted of weakly coupled viscid-inviscid methods. While good results have been obtained via these methods, a comprehensive analysis of the force characteristics of multiple slot/flap airfoils requires an analysis method that accounts for the strongly coupled nature of the different flow regimes.

Therefore, a two-dimensional Navier-Stokes solver with imbedded jet characteristics is appropriate to produce simulations for both blown and nonblown airfoils, thus providing continuity of force predictions. Several of these solvers[20,21]

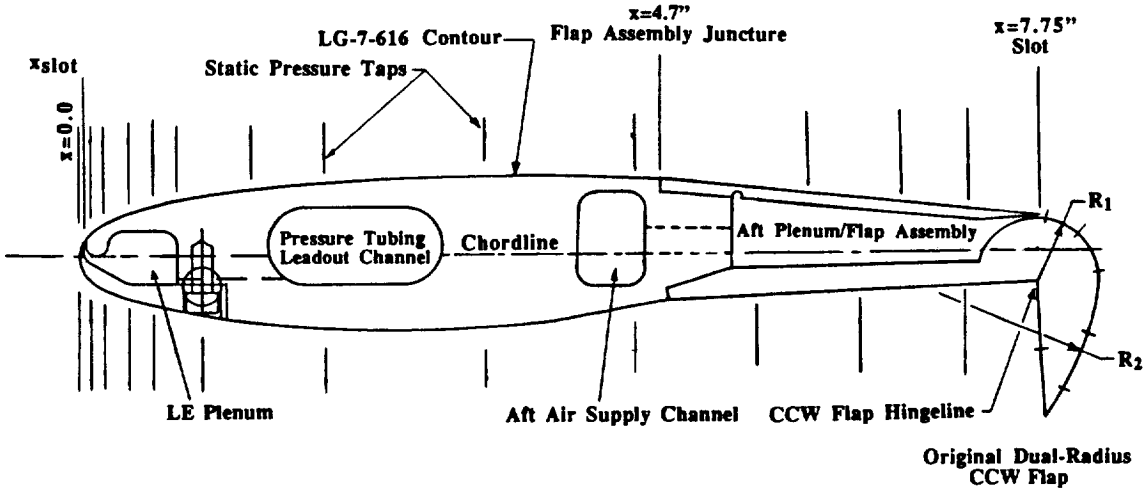

Fig. 12 Dual-slot, dual-radius CCW two-dimensional airfoil model.

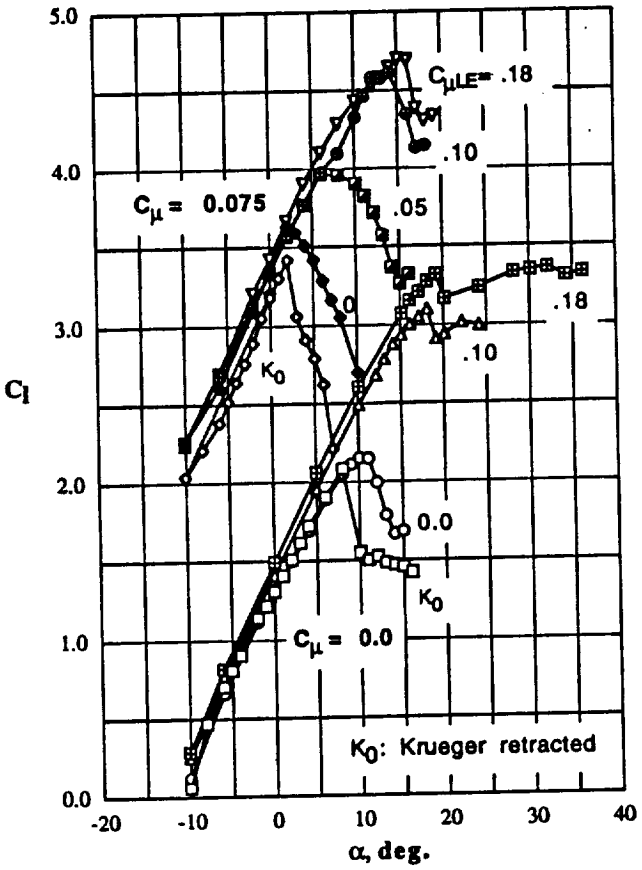

Fig. 13 Effectiveness of LE blowing in delaying stall onset.

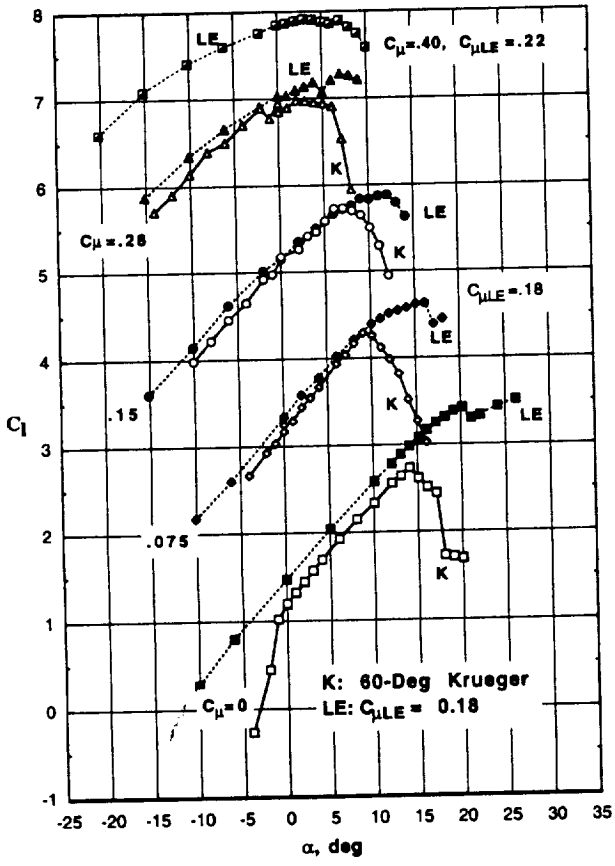

Fig. 14 LE blowing effectiveness compared to Krueger flap, $C_{\mu LE}$ = 0.18.

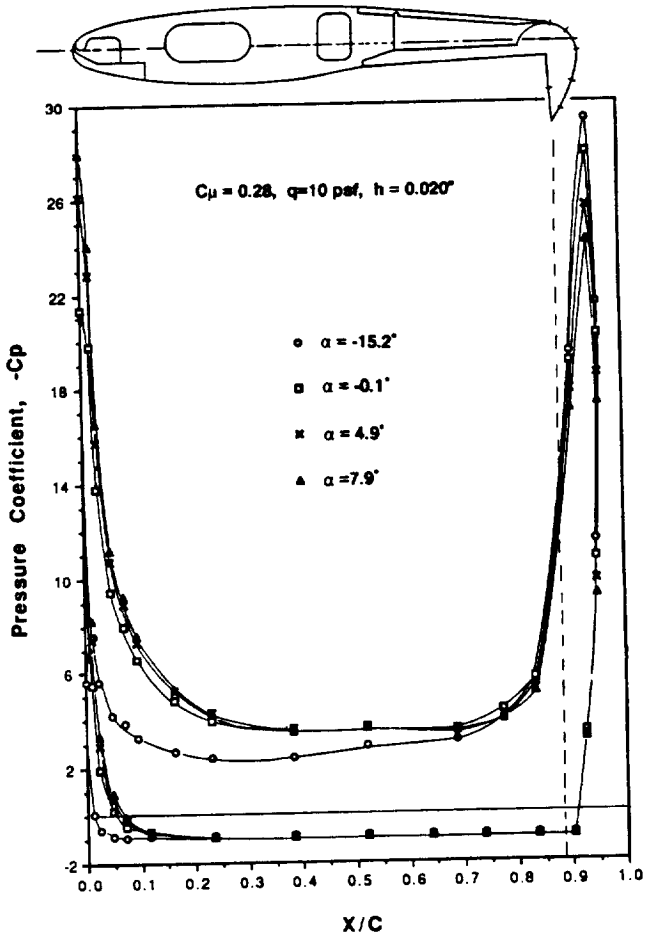

Fig. 15 Chordwise static pressure distributions for dual-slot, dual-radius CCW airfoil with $C_{\mu LE}$ = 0.10.

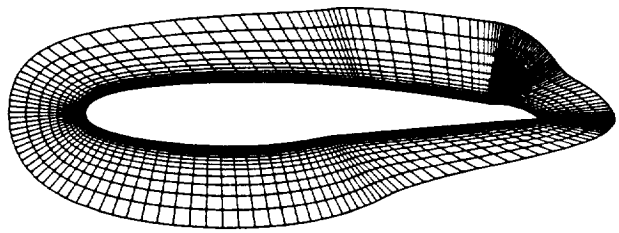

Fig. 16 Closeup of grid near the original dual-radius CCW airfoil at cruise condition.

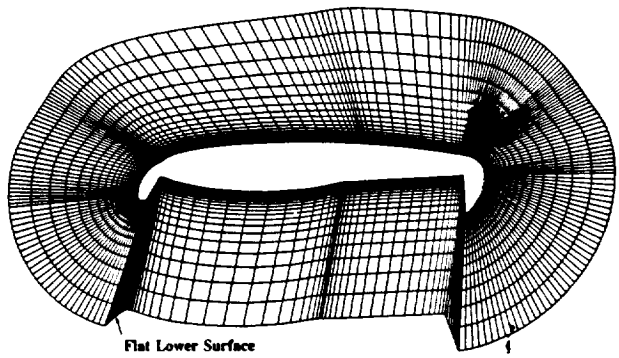

Fig. 17 Closeup of grid near the dual-radius CCW airfoil in the high-lift configuration.

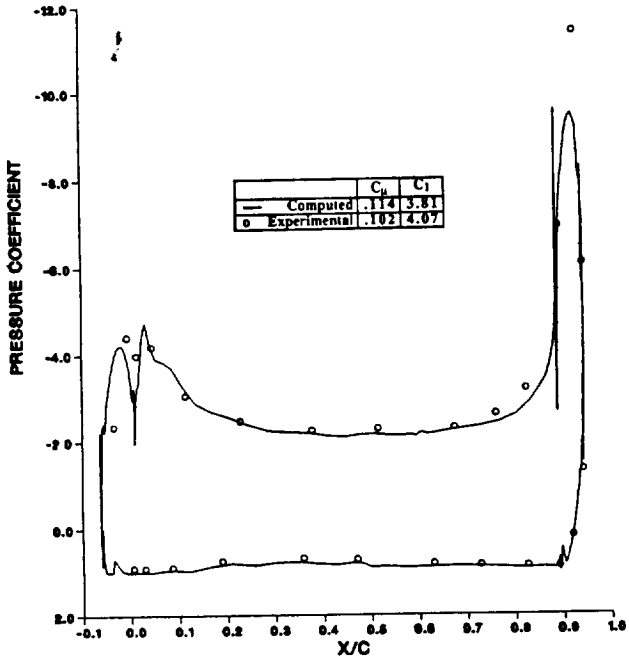

Fig. 18 Pressure distributions on dual-radius CCW airfoil with aft flap at 90 deg, Krueger flap at 60 deg, α = 0 deg, and C_μ = 0.10.

are currently available, including one developed by Georgia Tech[22] and Lockheed known as GT2DNSCC (Georgia Tech 2-D Navier-Stokes Circulation Control). The solver is based on a conventional two-dimensional Navier-Stokes method developed at Georgia Tech that has been applied and validated for a number of steady and unsteady applications[23,24] with conventional airfoil geometries. This Georgia Tech methodology is considered to be an industry standard in two-dimensional Navier-Stokes solvers, and is currently in use at several U.S. companies.[25]

The solver utilized in this project is based on GT2DNSCC, where the unsteady two-dimensional Reynolds-averaged, compressible Navier-Stokes equations are solved in a body fitted coordinate system using an alternating direction implicit (ADI) procedure. An in-depth discussion of the numerical details of the solver is given in Ref. 26. Two examples of the user-defined grid generation input are shown in Figs. 16 and 17, the first representing the clean cruise airfoil, and the second representing the CCW high-lift configuration, with the leading edge deployed.

The CFD simulations were first applied to locate the correct placement for the leading-edge slot. Positive angle-of-attack sweeps were performed analytically on the candidate airfoils at a Mach number of 0.1. By determining the chordwise location of the suction peaks at various angles of attack, the jet slot was located forward of the adverse pressure gradient to boost that suction peak and to avoid premature separation at higher angles of attack. The leading-edge design shown in Fig. 12 resulted from this analysis.

The CFD codes were also used to predict blown high-lift performance. Figure 18 shows a typical computed blown pressure distribution in comparison to measured data from the tunnel test. Agreement is quite good for this highly viscous flow case, with only small discrepancies noted due to slight variations in theoretical vs actual model geometry, actual blowing slot height when pressurized, and actual angle of attack.

One of the primary tasks of this study was to investigate the cruise performance of CCW airfoils since no compressible flow testing had been conducted. Cruise performance for the conventional and circulation control airfoils with flaps retracted was predicted for Mach numbers from 0.1 to 0.8, and drag polars were generated up through compressible speeds.

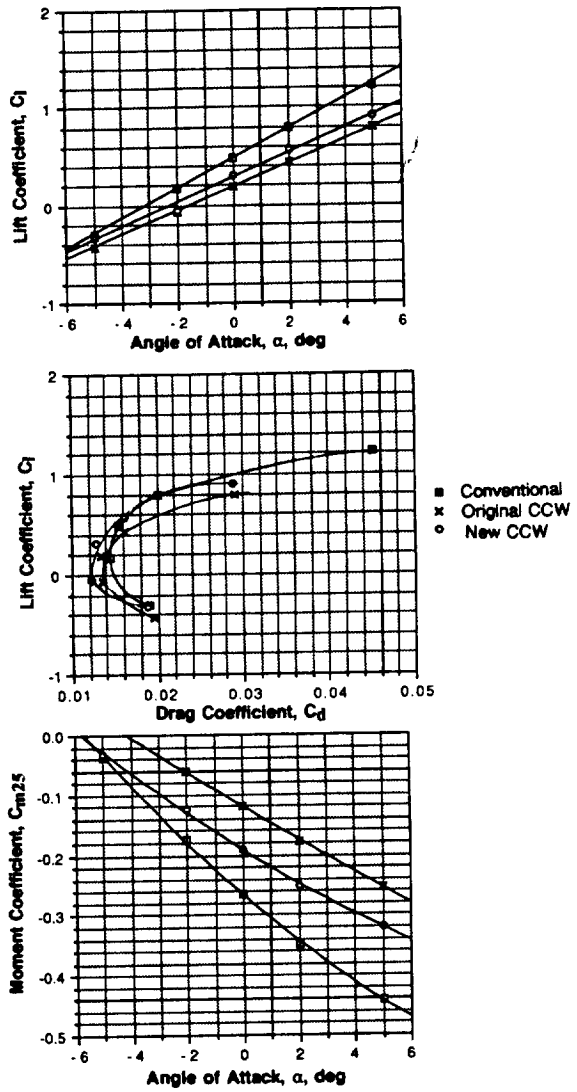

Fig. 19 Computed cruise performance characteristics at Mach-0.6 for conventional supercritical, original CCW, and modified CCW airfoils (no blowing).

A typical set of performance curves for unblown cruise configurations is shown for a Mach number of 0.6 in Fig. 19. The conventional airfoil (the upper configuration in Fig. 3) provides the best overall performance due to the thinner cusped trailing edge. The original CCW airfoil, which was based on previous CC airfoils and is shown in Fig. 16, had the poorest higher-speed performance. The new CCW airfoil, which incorporated many of the conventional airfoil shape features ahead of the slot and modified CC features downstream, showed a great improvement over the original CCW airfoil's characteristics. As angle of attack increases, the cruise performance of the CCW airfoils diminishes with respect to that of the conventional supercritical airfoil with aft camber. This is due to the effect of the discontinuity formed by the leading-edge blowing slot on the CC airfoils. It implies that the leading-edge slot should be as thin as possible. In actual use, it could be designed as a flexible lip, opened only when pressurized for low-speed, high-lift operation. At 4-deg angle of attack and lower, especially at lower Mach numbers, the cruise performance of the new CCW airfoil approaches or is equivalent to the original supercritical airfoil's performance.

Further details of this CFD analysis as well as additional details on test technique and results can be found in Ref. 27.

Conclusions

The above experimental and analytical results confirm the high-lift potential (C_l of 8 at α = 0 deg) of CCW advanced

airfoils aided by leading-edge blowing. Control of lift, drag, and pitching moments on these airfoils was provided by variations in blowing rate, angle of attack, LE or TE flap deflections, and blowing slot height. Extension of the computational analyses to cruise conditions indicates that new CCW airfoil shapes maintain good cruise characteristics at nonblown conditions, unlike previous larger TE radius blown airfoil geometries.

These results offer the potential for reduced complexity and lower terminal-area noise levels for subsonic transport aircraft equipped with CCW high-lift systems, and indicate similar payoffs for higher-speed transports. The results strongly suggest the potential of practical CCW transport configurations to provide the following capabilities, and it is thus recommended that further development be pursued:

1) CCW performance will greatly reduce takeoff and landing speeds, yielding reduced runway lengths and increased safety of flight in terminal areas.

2) Steep climbout and approach flight paths due to STOL capability can yield reduced noise exposure to surrounding communities.

3) Greatly increased liftoff gross weight and landing weight provided by smaller wing area will allow transport wings that are more optimized for cruise and greater fuel efficiency.

4) Pneumatic CCW configurations will greatly reduce high-lift system complexity, as will the combination of high-lift, roll-control, and direct-lift-control surfaces into a single multipurpose pneumatic wing/control surface.

Part II of this article discusses the application of circulation control technology to a typical subsonic transport aircraft, and further emphasizes these potential payoffs.

Acknowledgments

This project was sponsored by NASA Langley Research Center under Contract NAS1-19061. Work currently under way and just briefly reported on here is being funded under Grant NAG1-1517. The NASA Technical Monitor was Edgar G. Waggoner, Head, Subsonic Aerodynamics Branch, to whom the authors would like to express their appreciation for his support and encouragement.

References

[1]Englar, R. J., and Applegate, C. A., "Circulation Control-A Bibliography of DTNSRDC Research and Selected Outside References (Jan. 1969 to Dec. 1983)," David Taylor Naval Ship R&D Center Rept. (DTNSRDC) 84/052, Bethesda, MD, Sept. 1984.

[2]Englar, R. J., "Experimental Investigation of the High Velocity Coanda Wall Jet Applied to Bluff Trailing Edge Circulation Control Airfoils," Naval Ship R&D Center (NSRDC) Rept. 4708, Aero Rept. 1213, AD-A-019-417, Bethesda, MD, Sept. 1975.

[3]Jones, D. G., "Measurements of Wall Jet Development on a Circulation Control Aerofoil," Ph.D. Dissertation, Mechanical Engineering Dept., Univ. of California, Davis, Davis, CA, Jan. 1971.

[4]Englar, R. J., "Two-Dimensional Subsonic Wind Tunnel Tests of Two 15-Percent-Thick Circulation Control Airfoils," Naval Ship R&D Center, NSRDC TN AL-211, Bethesda, MD, Aug. 1971.

[5]Englar, R. J., "Development of the A-6/Circulation Control Wing Flight Demonstrator Configuration," David Taylor Naval Ship R&D Center, DTNSRDC Rept. ASED-79/01, Bethesda, MD, Jan. 1979.

[6]Williams, R. M., and Howe, H. J., "Two-Dimensional Subsonic Wind Tunnel Tests of a 20-Percent Thick, 5-Percent Cambered Circulation Control Airfoil," Naval Ship R&D Center, NSRDC TN AL-176, Bethesda, MD, Aug. 1970.

[7]Englar, R. J., "Low-Speed Aerodynamic Characteristics of a Small Fixed-Trailing Edge-Circulation Control Wing Configuration Fitted to a Supercritical Airfoil," David Taylor Naval Ship R&D Center, DTNSRDC Rept. ASED-81/08, Bethesda, MD, March 1981.

[8]Englar, R. J., and Huson, C. G., "Development of Advanced Circulation Control Wing High-Lift Airfoils," AIAA Paper 83-1847, July 1983; see also *Journal of Aircraft*, Vol. 21, No. 7, 1984, pp. 476–483.

[9]Wilson, M. B., and Von Kerczek, C., "An Inventory of Some Force Producers for Use in Marine Vehicle Control," David Taylor Naval Ship R&D Center, DTNSRDC-79/097, Bethesda, MD, Nov. 1979.

[10]Englar, R. J., Hemmerly, R. A., Moore, W. H., Seredinsky, V., Valckenaere, W. G., and Jackson, J. A., "Design of the Circulation Control Wing STOL Demonstrator Aircraft," AIAA Paper 79-1842, Aug. 1979.

[11]Pugliese, A. J., and Englar, R. J., "Flight Testing the Circulation Control Wing," AIAA Paper 79-171, Aug. 1979.

[12]Englar, R. J., and Williams, R. M., "Test Techniques for High Lift Two-Dimensional Airfoils with Boundary Layer and Circulation Control for Application to Rotary Wing Aircraft," *Canadian Aeronautics and Space Journal*, Vol. 19, No. 3, 1973, pp. 93–103; see also Naval Ship R&D Center, NSRDC Rept. 4645, Bethesda, MD, July 1975.

[13]Englar, R. J., Schuster, D. M., and Ford, D. A., "Experimental Evaluations of the Aerodynamics of Unlimited Racing Hydroplanes Operating In and Out of Ground Effect," Society of Automotive Engineers Paper 901869, Oct. 1990; see also *SAE 1990 Transactions, Journal of Aerospace*, Sec. 1, Vol. 99, Pt. 2, 1991, pp. 1615–1624.

[14]Englar, R. J., "The Application of Circulation Control Pneumatic Technology to Powered-Lift STOL Aircraft," Society of Automotive Engineers Paper 872335, Dec. 1987; see also *Proceedings of the International Powered Lift Conference* (Santa Clara, CA), 1988, pp. 357–369 (SAE P-203).

[15]Kohlman, D. L., *Introduction to V/STOL Airplanes*, Iowa State Univ. Press, Ames, IA, 1981, pp. 123–165.

[16]Gibbs, E. H., and Ness, N., "Analysis of Circulation Controlled Airfoils," West Virginia Univ. Dept. of Aerospace Engineering, Rept. TR-43, Morgantown, WV, June 1975.

[17]Dvorak, F. A., and Kind, R. J., "Analysis Method for Viscous Flow over Circulation-Controlled Airfoils," *Journal of Aircraft*, Vol. 16, No. 1, 1979, pp. 23–28.

[18]Dvorak, F. A., and Choi, D. H., "Analysis of Circulation Controlled Airfoils in Transonic Flow," *Journal of Aircraft*, Vol. 20, No. 4, 1983, pp. 331–337.

[19]Dash, S. M., and Wolf, D. E., "Viscous/Inviscid Analysis of Curved Wall Jets: Part 1-Inviscid Shock Capturing Model (SCIPWJET)," SAI/PR TR-5, Princeton, NJ, Sept. 1982.

[20]Berman, H. A., "A Navier-Stokes Investigation of a Circulation Control Airfoil," AIAA Paper 85-0300, Jan. 1985.

[21]Pulliam, T. H., Jesperson, D. C., and Barth, T. J., "Navier-Stokes Computations for Circulation Controlled Airfoils," AIAA Paper 85-1587, July 1985.

[22]Shrewsbury, G. D., "Analysis of Circulation Control Airfoils Using an Implicit Navier-Stokes Solver," AIAA Paper 85-0171, Jan. 1985.

[23]Wu, J.-C., "A Study of Unsteady Turbulent Flow Past Airfoils," Ph.D. Dissertation, Georgia Inst. of Technology, Atlanta, GA, June 1988.

[24]Sankar, N. L., and Tang, W., "Numerical Solution of Unsteady Viscous Flow Past Rotor Sections," AIAA Paper 85-0129, Jan. 1985.

[25]Smith, M. J., and Hassan, A. H., "Improvement to Interactive Two Dimensional Rotor Section Design," American Helicopter Society Vertical Lift Aircraft Design Conf., San Francisco, CA, Jan. 1990.

[26]Shrewsbury, G. D., "Dynamic Stall of Circulation Control Airfoils," Ph.D. Dissertation, Georgia Inst. of Technology, Atlanta, GA, Nov. 1990.

[27]Englar, R. J., Smith, M. J., Kelley, S. M., and Rover, R. C., III, "Development of Circulation Control Technology for Application to Quiet Advanced Subsonic Transport Aircraft," Georgia Tech. Research Inst. Rept. A-8612-006, Dec. 1991.

JOURNAL OF AIRCRAFT
Vol. 31, No. 5, Sept.–Oct. 1994

Application of Circulation Control to Advanced Subsonic Transport Aircraft, Part II: Transport Application

Robert J. Englar,* Marilyn J. Smith,† Sean M. Kelley,‡ and Richard C. Rover III‡
Georgia Tech Research Institute, Atlanta, Georgia 30332

An experimental/analytical research program was undertaken to develop advanced versions of circulation control wing (CCW) airfoils and to address specific issues related to the application of these blown high-lift devices to subsonic transport aircraft. The primary goal was to determine the feasibility and potential of these pneumatic configurations to increase high-lift system performance in the terminal area while reducing system complexity and aircraft noise. A four-phase program was completed, including 1) experimental development and evaluation of advanced CCW high-lift configurations; 2) development of effective pneumatic leading-edge devices; 3) computational evaluation of CCW airfoil designs plus high-lift and cruise capabilities; and 4) the investigation of the terminal-area performance of transport aircraft employing these airfoils. The first three phases were presented in Part I of this article. This segment, Part II, describes the fourth phase of the program. Experimental lift coefficient values approaching 8.0 at zero incidence were demonstrated by two-dimensional CCW configurations and were reported in Part I. These were used to predict 70–80% reductions in takeoff and landing distances for a three-dimensional advanced subsonic transport configuration employing a simplified pneumatic high-lift system. These results and the methodology used to obtain them will be presented in greater detail in the following discussions.

Nomenclature

a_x = longitudinal acceleration
C_D = wing or aircraft drag coefficient
C_d = airfoil drag coefficient
C_L = wing or aircraft lift coefficient;
$C_{L\,app}$ = approach lift coefficient
C_l = airfoil lift coefficient
C_μ = jet momentum (blowing) coefficient
c = airfoil chord length
c_f = flap chord length
EKv = kinetic energy, vertical component
h = height above ground
$\dot{m}$ = blowing jet mass flow rate
q = freestream dynamic pressure
r = CCW flap radius
S = wing planform area
S_{eff} = effective blown planform area
S_g = ground roll distance
S_{50} = distance over 50-ft obstacle
T = ambient temperature
T = engine installed thrust
V = freestream velocity
V_{app} = approach velocity
V_j = isentropic jet velocity
V_{LO} = liftoff velocity
W_A = engine airflow
$W_{A\,core}$ = engine core airflow
W_F = engine fan airflow
x = horizontal distance over ground
α = angle of attack
α_{stall} = stall angle of attack
Δ = delta, change in
δ_f = flap deflection angle
γ = climb angle

Subscripts
2-D = two dimensional
3-D = three dimensional

Presented as Paper 93-0644 at the AIAA 31st Aerospace Sciences Meeting and Exhibit, Reno, NV, Jan. 11–14, 1993; received April 27, 1993; revision received Feb. 25, 1994; accepted for publication March 7, 1994.

*Senior Research Engineer, Aerospace Sciences Laboratory. Associate Fellow AIAA.
†Senior Research Engineer, Aerospace Sciences Laboratory. Senior Member AIAA.
‡Cooperative Student, Aerospace Sciences Laboratory.

Introduction

BASED on existing data,[1] pneumatic high-lift airfoils appear to offer significant payoffs in the design and development of next-generation subsonic transport aircraft. Both ground and flight experimental investigations have previously shown that a specific type of blown airfoil known as the circulation control wing (CCW) can greatly augment the high-lift capabilities provided by conventional mechanical flaps. References 1–12 provide summaries of some of these developments and include verification of CCW airfoil sections generating very high lift at low blowing rates. They also discuss successful CCW applications to and flight tests on fixed-wing short takeoff and landing (STOL) and rotary-wing vertical takeoff and landing (VTOL) aircraft. The CCW concept employs tangential blowing over round or near-round trailing edges to pneumatically replace multielement mechanical flaps. Here, the lack of a sharp trailing edge avoids the Kutta condition requirement that the stagnation streamline depart the airfoil at the trailing edge. The jet turning action does, in fact, produce a pneumatic cambering device. The result is very high-lift generation, with two-dimensional lift coefficients greater than 7.0 being generated at 0-deg angle of attack.[2] Lift augmentation ($\Delta C_l/C_\mu$) as high as 80 or more has been reported in Refs. 1 and 6. The driving parameter is the momentum coefficient, defined for three-dimensional wings as

$$C_\mu = \dot{m}V_j/qS \tag{1}$$

In addition, high-lift system complexity can be reduced by substituting simplified pneumatic components for mechanical flaps, tracks, and actuators. Figure 1 (from Part I of this article) shows a no-moving-parts CCW trailing edge applied to a NASA supercritical airfoil section.[7,8] Not only are the

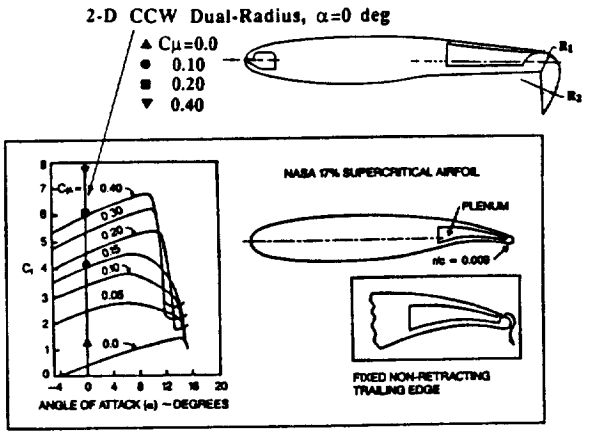

Fig. 1 Comparison of two-dimensional dual-radius CCW/supercritical airfoil with monoelement round CCW/supercritical high-lift system.

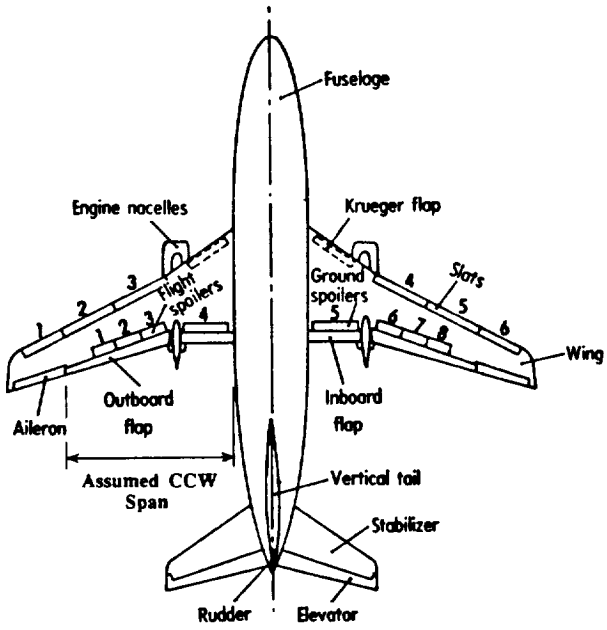

Fig. 2 High-lift and control surfaces for conventional B737 (from Ref. 13) and flap span for B737/CCW aircraft.

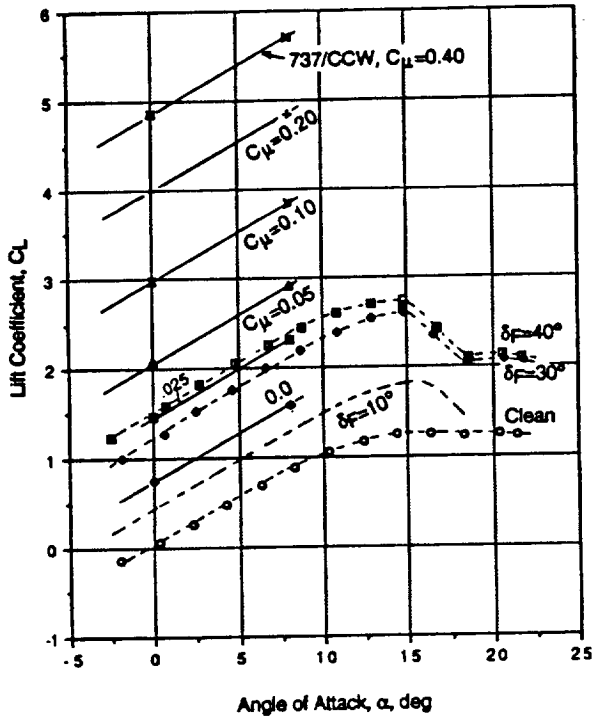

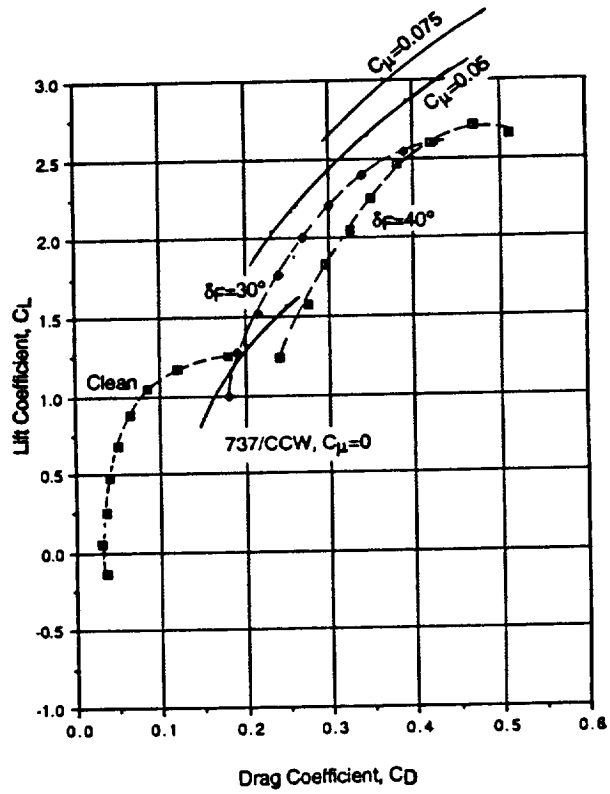

Fig. 3 One-eighth-scale wind-tunnel lift and drag data for B737 aircraft (from Ref. 13), and predicted B737/CCW data (90-deg CCW flap, 60-deg Krueger flap).

conventional leading-edge and trailing-edge components eliminated, but the resulting lift values (at zero incidence and up through maximum C_l) are quite significant. As this figure shows, CCW airfoils applicable to transports typically generated C_l values of 6 to 7, equal to or exceeding the high-lift potential of even the most complex multielement mechanical flap airfoils. Pneumatic concepts can further simplify transport aircraft wings by eliminating the need for mechanical leading-edge devices as well as mechanical-roll-control or direct-lift-control surfaces.[9] In Part I of this article, an advanced dual-radius CCW with a pneumatic leading edge was developed that generated lift coefficients approaching 8 at 0-deg incidence, which represents as much as 30–35% increase in lift over the prior CCW results. This airfoil is also shown in Fig. 1, where the resulting improvement in lift performance is seen as the solid symbols. Since blowing behaves as a pneumatic flap, lift curves through these α = 0-deg points will be parallel to curves at constant flap angles δ_f, with $C_{L\,max}$ a function of the leading-edge device effectiveness.

While the high-lift and simplifying capabilities of these CCW devices have been confirmed in experimental programs and in actual flight demonstrations,[10,11] specific application-related issues need to be addressed to take maximum advantage of these pneumatic benefits. The two-dimensional research discussed in Part I developed new versions of the CCW pneumatic airfoil. The present research project, Part II, was undertaken to resolve these application issues in order to make pneumatic airfoil technology available for use in next generation transports or on retrofits of existing aircraft. Specific issues to be addressed in Part II include analytically applying

Table 1 Aerodynamic characteristics of the conventional B737 aircraft

Condition	Flap	α	C_L	C_D
Takeoff ground roll	30 deg	1.0 deg	1.320	0.196
Liftoff	30 deg	8.0 deg	2.130	0.288
Landing ground roll	40 deg	1.0 deg	1.640	0.275
Approach	40 deg	6.0 deg	2.175	0.342

Table 2 B737-100 terminal area operating parameters

Empty weight	62,000 lb
Typical gross weight	111,000 lb
Maximum landing weight	101,000 lb
Typical landing speed	144 mph
FAA takeoff field length	4,300 ft
FAA landing field length	4,000 ft

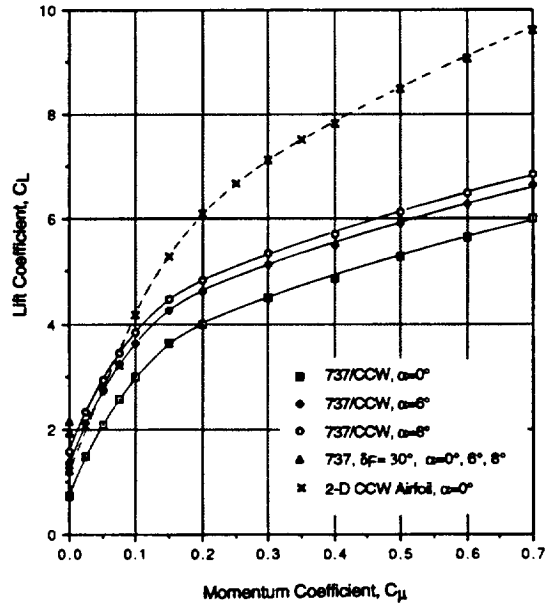

Fig. 4 B737/CCW aircraft lift due to blowing (90-deg CCW flap, 60-deg Krueger flap).

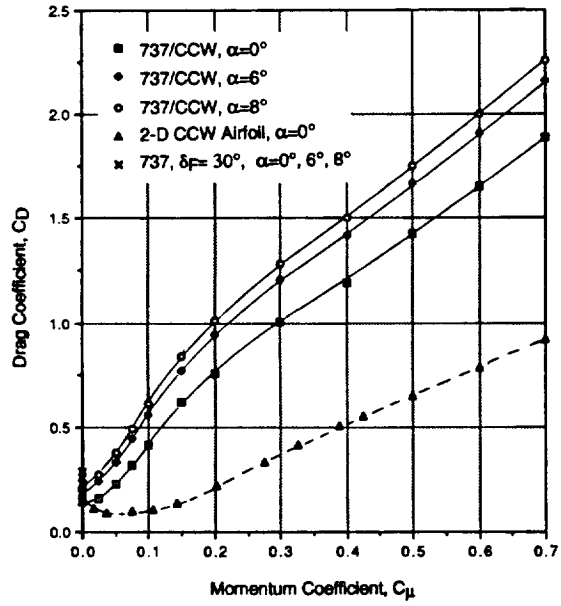

Fig. 5 B737/CCW aircraft drag due to blowing (90-deg CCW flap, 60-deg Krueger flap).

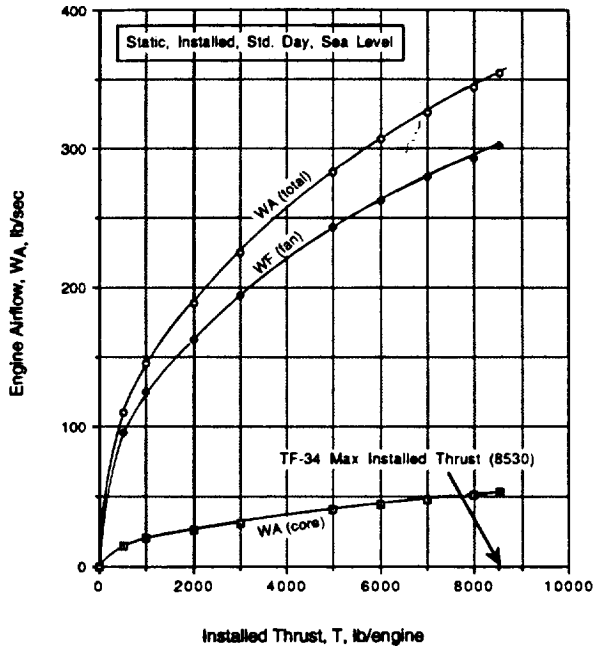

Fig. 6 TF-34 thrust and airflow characteristics.

the two-dimensional results of Part I to a postulated advanced subsonic transport, and investigating system performance for that aircraft employing a CCW high-lift system. Results of these investigations will be presented in the following sections.

Investigation of CCW System Performance

Results of the two-dimensional evaluations presented in Part I of this study were incorporated into the design of an advanced CCW high-lift system for a subsonic commercial transport aircraft. This required prediction of the blown aircraft's high-lift capabilities with available or postulated air sources powering the system, and employing appropriate analytical routines to predict the takeoff and landing performance. These analyses had to take into account any new restrictions placed on blown high-lift aircraft if these deviated from conventional mechanical systems. The following sections discuss generation of the aircraft high-lift characteristics, prediction of the associated terminal area performance of the modified commercial transport, and discussion of resulting issues relevant to blowing system integration into the CCW aircraft.

Transport Aerodynamic Characteristics

The Boeing 737-100, a twin-engined commercial transport (hereafter referred to as B737) was chosen as a comparative sample case to investigate potential gains to be realized from the CCW application. This aircraft was especially convenient as NASA Langley Research Center currently operates that configuration (Research Aircraft NASA 515) in its ongoing Subsonic Transport High-Lift Flight Research program. In its production version, it employs a triple-slotted mechanical flap with leading-edge slats and Krueger flaps, thus placing it near the best of the mechanical systems shown in Fig. 1 of the Part I article. Figure 2 shows the arrangement of these mechanical components on the B737 wing, and the comparable CCW system proposed for the same span. (In actual application, the authors would propose full-span blowing all the way to the outboard aileron edge, with roll control by means of differential blowing, but that would have been an unfair comparison to the actual mechanical flaps in this case.)

In the absence of actual full-scale flight test data for this aircraft, NASA Langley personnel supplied Ref. 13, which provided B737 baseline geometry and aerodynamic characteristics from $\frac{1}{8}$-scale wind-tunnel results. These model data,

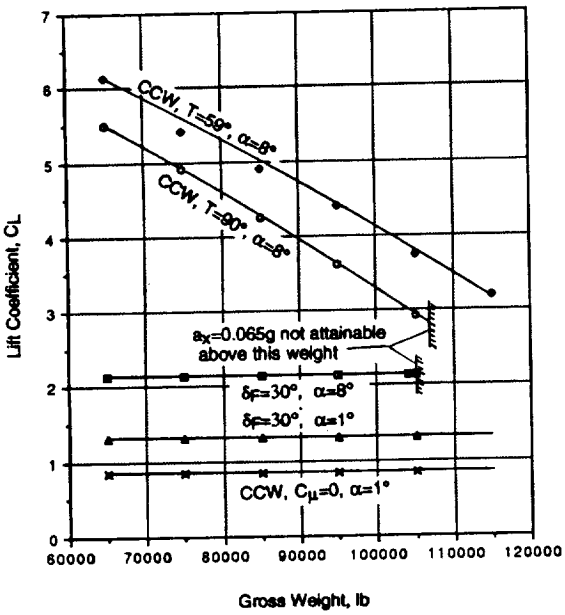

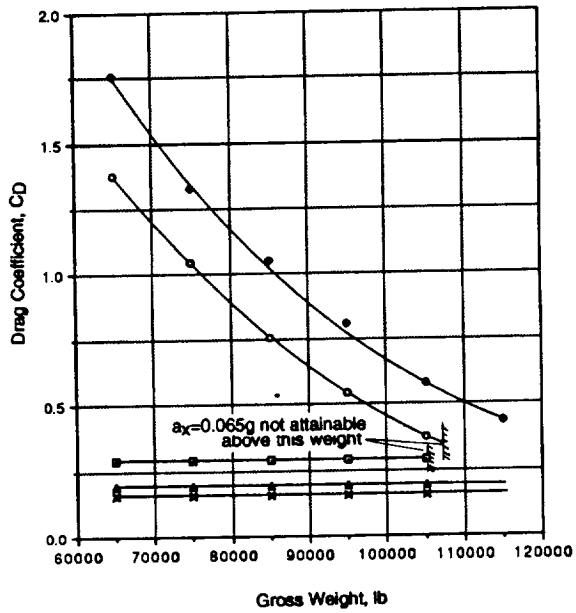

Fig. 7 Lift available at takeoff for B737 and B737/CCW aircraft (90-deg CCW, 60-deg Krueger), sea level.

shown in Fig. 3, were used to represent the B737-100 in the following analyses. Also shown are predicted characteristics of the CCW version of this aircraft (to be discussed below). The following should be noted: 1) the Fig. 3 wind-tunnel data are untrimmed and out of ground effect, and 2) Reynolds number corresponds to q = 30 psf on the $\frac{1}{4}$-scale model, not full-scale.

Critical to takeoff and landing performance is the operational angle of attack. Using FAA guidelines for commercial transports (FAR Part 25, Ref. 14), the takeoff velocity should be 1.10 × V_{stall}, and the touchdown velocity 1.15 × V_{stall}. If the takeoff flap setting is assumed as 30 deg, and the landing flap as 40 deg on the B737 aircraft, takeoff will occur at α = 8 deg, and landing at α = 6 deg. This corresponds to the aerodynamic characteristics for the conventional aircraft (from Fig. 3), shown in Table 1.

It is realized that actual B737 takeoff is probably at a lesser flap setting angle than 30 deg (possibly 10 deg or so), but wind-tunnel data for that flap setting was not available. The 10-deg lift curve is approximated in Fig. 3, but drag was not

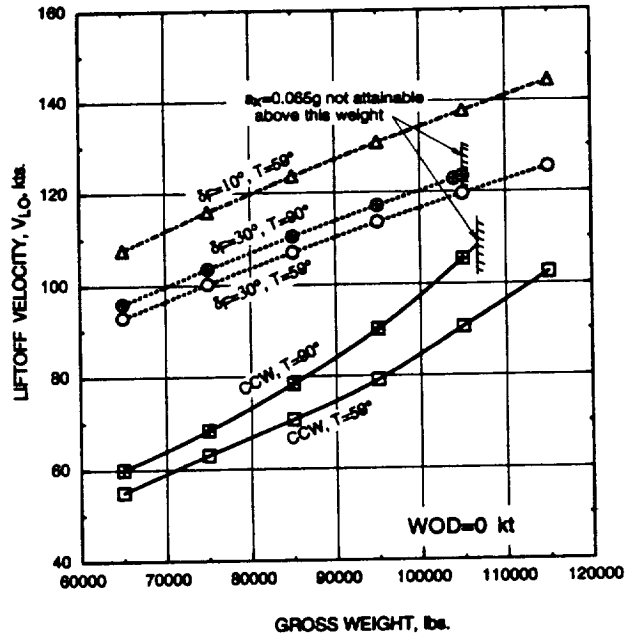

Fig. 8 Predicted liftoff velocities for B737 and B737/CCW.

easily interpolated. For the takeoff and the climbout calculations, the shortened ground roll due to increased lift at 30 deg rather than 10 deg will be offset somewhat by the increased drag. The main intent here is to compare the takeoff trends from a conventional flap to those for the CCW configuration. Pertinent B737-100 operational data obtained from Ref. 15 are shown in Table 2.

B737/CCW Aerodynamic Characteristics

In the absence of wind-tunnel evaluations of a three-dimensional B737/CCW model, an existing semiempirical method[10,16,17] was used to convert data for the two-dimensional dual-radius CCW airfoil with the Krueger leading-edge flap (Figs. 3, 11, and 14 from Part I) into three-dimensional finite-wing data for the B737, spanning the same portion of the wing as the existing mechanical flaps and leading-edge devices, Fig. 3. This method adjusts the two-dimensional data for sweep, taper ratio, aspect ratio, partial-span flaps, and three-dimensional lift curve slope, and provides an increment in lift at α = 0 deg, which is then added to the clean aircraft lift at zero incidence:

$$C_{L_{blown}} = C_{L_{clean}} + \Delta C_{L_{CCW}} = 0.04 + 0.5804\Delta C_{l_{CCW}} \quad (2)$$

Here, all input two-dimensional values ($C_{l_{CCW}}$) are the α = 0-deg value at a given C_μ for the flap at 90 deg (see Fig. 1), and the clean B737 value (C_L = 0.04) came from Fig. 3. An entire family of these values will exist, as both blowing and incidence are variable. The blowing-dependent values of $\Delta C_{l_{CCW}}$ came from the two-dimensional data (such as Fig. 6 of Part I) corresponding to the appropriate two-dimensional C_μ, based on only the blown wing area S_{eff}:

$$C_{\mu_{2\text{-}D}} = C_{\mu_{3\text{-}D}} S/S_{eff} \quad (3)$$

The lift due to incidence is derived by assuming (based on much past experience) that the blown lift curves will parallel the mechanical-flap curves for the same affected wing area. Using this procedure, the lift data of the B737/CCW configuration at α = 0, 6, and 8 deg were generated and plotted in Fig. 4. The original two-dimensional data at α = 0 deg are shown for comparison. These B737/CCW lift curves are also plotted in Fig. 3 for comparison to the baseline B737. The 6-

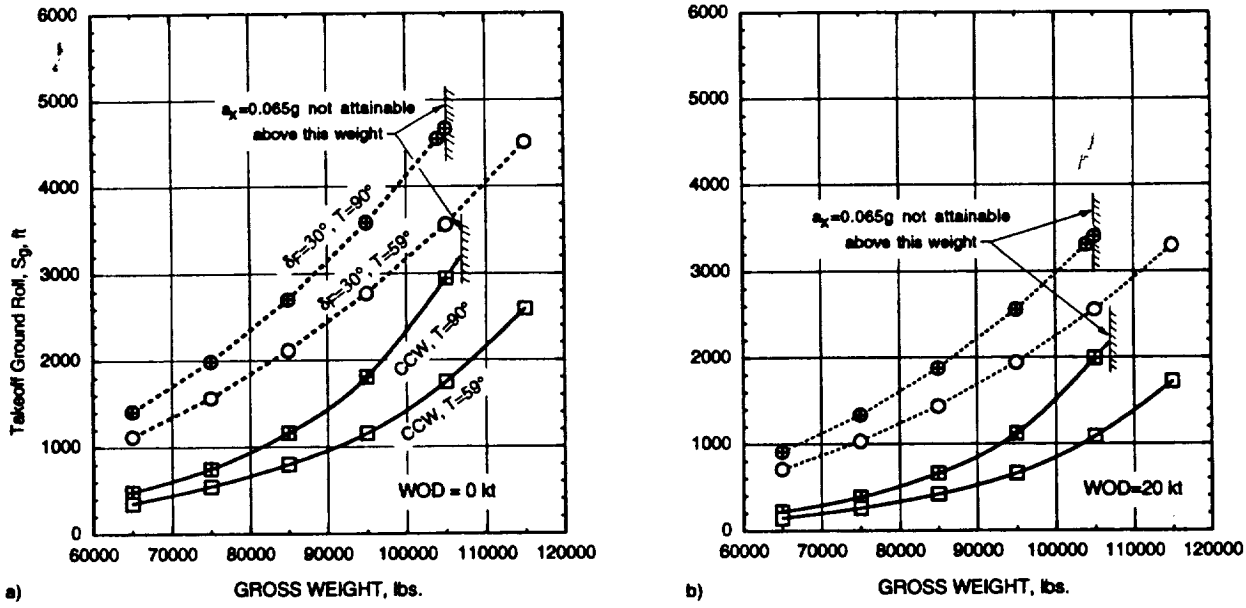

Fig. 9 Predicted ground rolls for B737 and B737/CCW aircraft, sea level: a) no head wind (WOD = 0 kt) and b) 20-kt head wind.

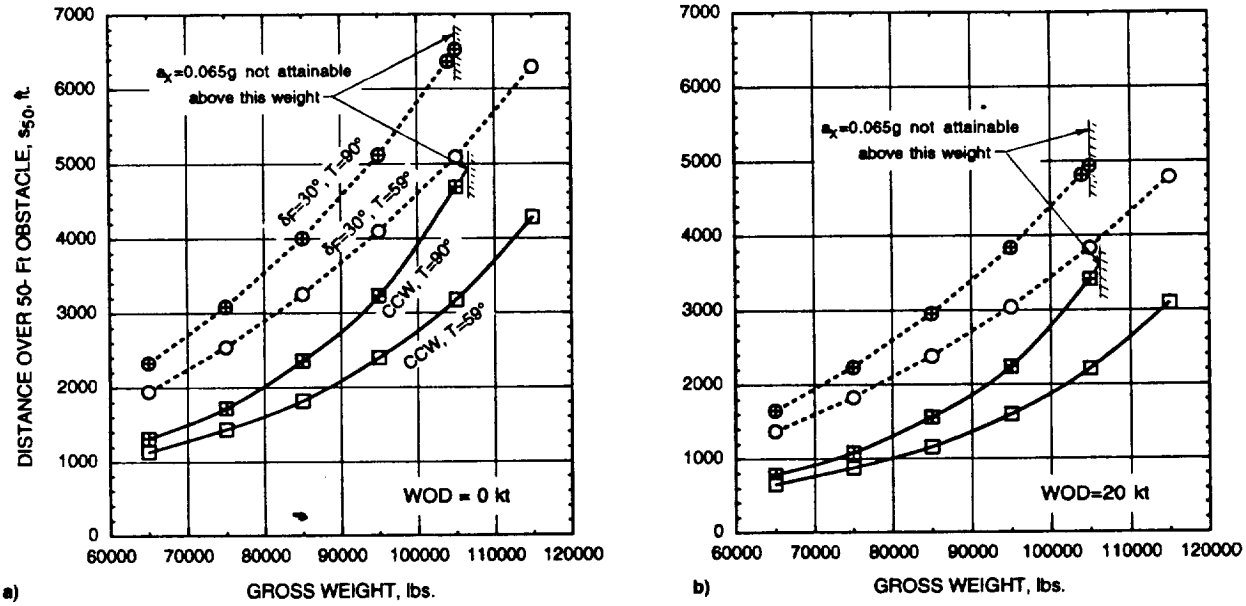

Fig. 10 Predicted distance over a 50-ft obstacle for B737 and B737/CCW: a) no head wind (WOD = 0 kt) and b) 20-kt head wind.

and 8-deg angle-of-attack values are retained as the landing and takeoff values of the B737/CCW aircraft to make results directly comparable to the conventional B737.

The blown drag was determined using the same semiempirical method,[10,16,17] and is described in more detail in Ref. 18:

$$C_D = C_{D_{\text{clean}}} + C_{D_{\text{profile}}} + C_{D_{\text{blowing}}} + C_{D_{\text{incidence}}} \qquad (4)$$

where $C_{D_{\text{clean}}}$ is the zero-incidence cruise drag of the baseline B737, and $C_{D_{\text{profile}}}$ is derived from the two-dimensional measured drag at $\alpha = 0$ deg corrected for area S/S_{eff} and three-dimensional planform effects, just as $C_{L_{\text{blown}}}$ was. Figure 5 shows the resulting drag for the two-dimensional airfoil at $\alpha = 0$ deg, and for the three-dimensional B737 and B737/CCW aircraft at $\alpha = 0$, 6, and 8 deg. Representative drag polars for the CCW aircraft with 90-deg flap deflection, both with and without blowing, have been added to those of the conventional aircraft in Fig. 3. These data are sufficient to predict takeoff and landing performance once the aircraft engine characteristics are known.

Engine Characteristics with Blowing

Detailed engine characteristics for the B737-100's JT8D-15 turbofan engines with blowing were not available at the time of these initial predictions. It was thus decided to scale the characteristics of an existing similar engine, the TF-34 turbofan, for which satisfactory performance data was known.[17,19] At this point, it was assumed that bleed would be taken directly from the engine to avoid requiring a separate auxiliary power unit (APU). The JT8D-15 engine characteristics were scaled from the TF-34, using a 1.67116-scale factor based on rated thrust and an 8% installation thrust loss, which were applied to the data of Fig. 6. To avoid larger thrust loss due to core bleed, it was further assumed that only airflow from the fan would be used to power the CCW on takeoff and landing, and that the maximum pressure ratio available was

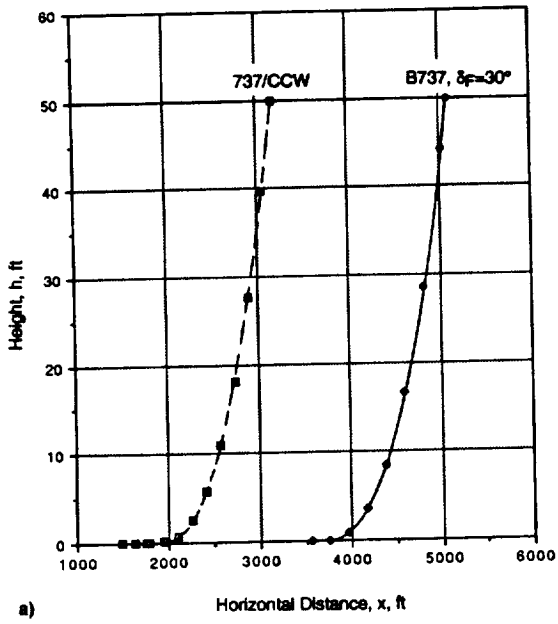

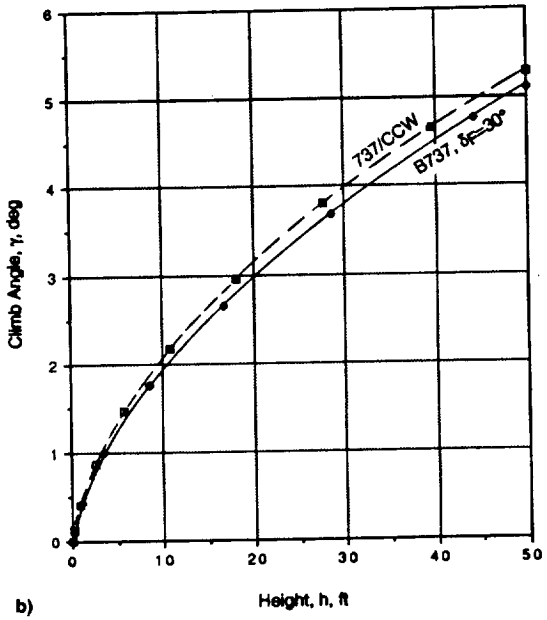

Fig. 11 Predicted takeoff flight paths for B737 and B737/CCW aircraft: a) flight path and b) climb angle. Gross weight = 105,000 lb, T = 59°F, WOD = 0 kt.

1.5. Thrust loss due to fan bleed was assumed to be equal to the percent of airflow removed from the fan (i.e., 5% fan airflow removal resulted in 5% thrust loss). Further details of engine bleed, ram drag accounting, etc., are provided in Ref. 18.

B737 and B737/CCW Takeoff Performance

To analyze the effects of pneumatic high-lift systems on the takeoff performance of advanced transport aircraft, an existing STOL takeoff performance routine developed during the A-6/CCW STOL Demonstrator program[10,16,17] was revised and updated. Since takeoff and landing conditions are not known a priori for blown aircraft (i.e., C_L and C_D are dependent on C_μ, which is dependent on attainable liftoff dynamic pressure, which is dependent on weight, blowing momentum, and available C_L and C_D, which are dependent on C_μ, etc.), an iterative routine is required. This is further complicated by additional requirements such as one-engine-out on takeoff, takeoff acceleration required, climbout gradients,

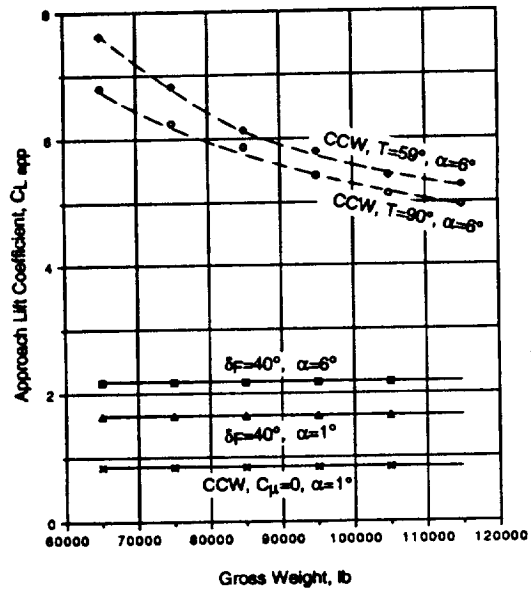

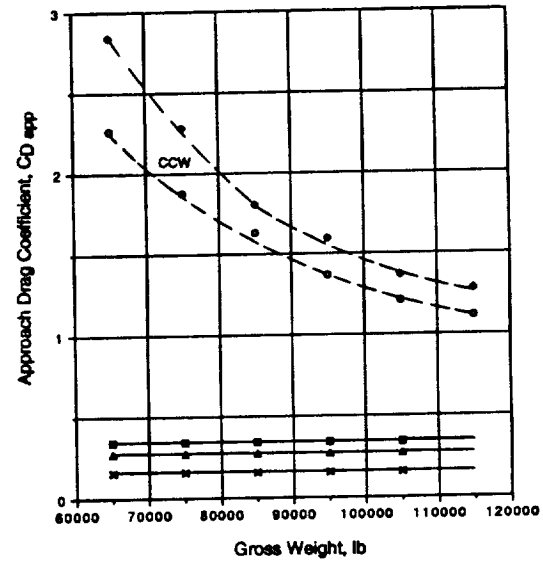

Fig. 12 Available lift for B737 (40-deg flap) and B737/CCW (90-deg CCW flap, 60-deg Krueger flap) at approach incidence down a 4-deg glide slope and during ground roll.

etc. The existing numerical routine was verified for a Navy A-6 aircraft using existing Navy operational data sets and charts.[16,17]

Figures 7–11 show typical results of the effects of blowing on B737/CCW available lift, liftoff speeds, and ground rolls. In Fig. 7, the takeoff lift and drag coefficients do not vary with weight for the conventional B737 during ground roll (α = 1 deg), or at liftoff (α = 8 deg), nor for the B737/CCW during unblown ground roll. However, available C_μ, and thus the blown C_L and C_D, do vary with weight and available airflow momentum, which thus affects liftoff speed. Notice that at lighter weight, the available C_L from blowing is as much as three times that of the baseline B737, and 75% greater at the heavier weights. Figure 8 presents the corresponding reductions in liftoff speed due to CCW, ranging between 15–40% (depending on weight) of the speeds of the B737 with 30-deg flap deflection. Also shown is the approximate curve for the 10-deg flap setting. These significant reductions in liftoff speed were produced by using only engine fan bleed on an otherwise standard B737 to power a CCW high-lift system. Figures 9 and 10 depict the resulting reductions in takeoff ground roll distance and distance over a 50-ft obstacle,

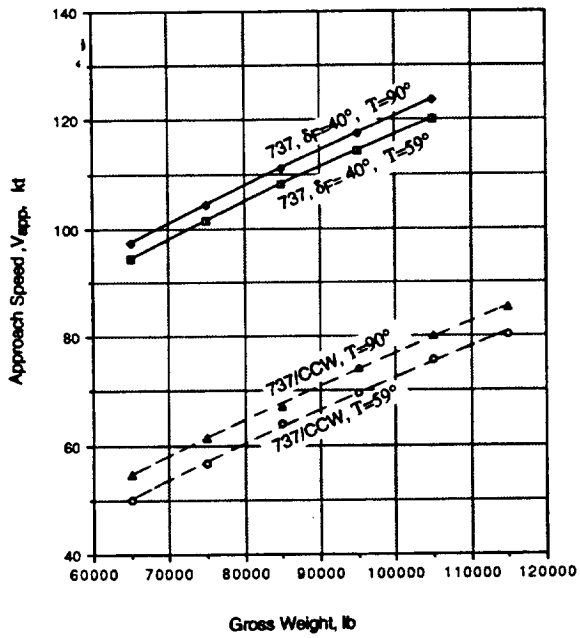

Fig. 13 Predicted reduction in equilibrium approach speeds down at 4-deg glide slope for B737 and B737/CCW aircraft at sea level (90-deg CCW flap, 60-deg Krueger flap).

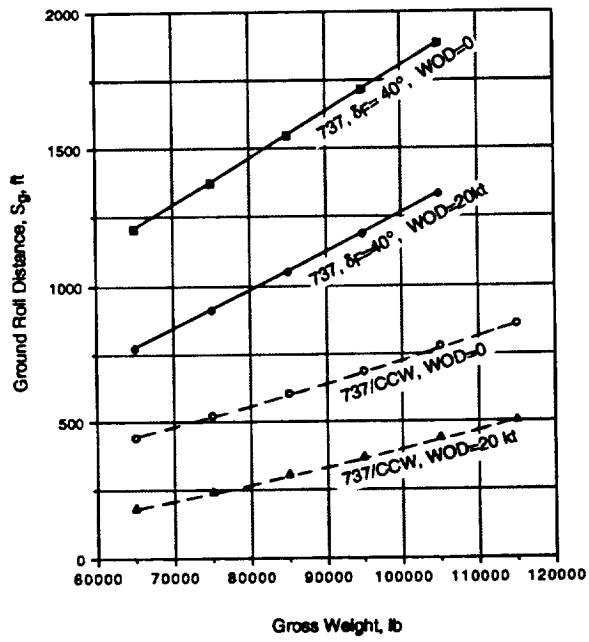

Fig. 14 Predicted landing ground roll for B737 and B737/CCW aircraft at sea level, T = 59°F.

and how those parameters are affected by temperature and head wind [labeled wind-over-deck (WOD)]. Relative to the conventional B737, the CCW version reduced ground roll distances from 37 to 80% (with light weight, 20-kt head wind, and T = 59°F being the best conditions), and reduced distance over the 50-ft obstacle by 27–74%. While a flap angle of less than 30 deg might be expected to increase the conventional aircraft's performance by reducing the drag, the same would be expected for a takeoff version of the B737/CCW with a flap deflection less than 90 deg.

Note the limitations placed on performance by the requirement that available blowing be reduced (to reduce drag and increase thrust) until the available horizontal acceleration at liftoff is at least 0.065 g. This results from a Navy operational limitation to account for the possibility of one-engine-out at liftoff, and is retained here as a conservative measure. It should eventually be replaced by the commercial aviation equivalent limitation. Figure 11 shows the climb angle and flight path after liftoff for a typical 105,000-lb B737 and B737/CCW, both with no head wind. Blowing was not reduced after the CCW aircraft's liftoff, and its flap deflection remained at 90 deg; thus that aircraft still experienced high-induced drag during climbout. The B737's flap remained at 30 deg. Nevertheless, the CCW climb angle at 50 ft is virtually the same as the B737, whereas the CCW aircraft traversed only 60% of the ground distance. This performance could be improved if the bleed rate were reduced as the aircraft was climbing, i.e., to maintain a constant rate of climb.

B737 and B737/CCW Landing Performance

To continue analysis of the effects of pneumatic high-lift systems on the terminal area performance of advanced transport aircraft, an existing STOL landing performance routine developed during the A-6/CCW STOL Demonstrator program[10.16] was also revised and updated. This existing landing program had also been verified for a Navy A-6 aircraft.[10.17] As was the case for takeoff, landing conditions for blown aircraft were also not known a priori. An iterative routine was again required. This landing analysis was further complicated by additional requirements imposed, such as no acceleration down the glide slope, maximum allowable rate of sink at touchdown, etc. Figures 12–16 show typical results of the effects of blowing, head wind, and temperature on available aerodynamic coefficients, approach speed, and landing ground roll. There is a significant impact on landing performance produced by using only enough engine bleed to maintain equilibrium flight along the glide slope. Even so, increases in available lift for the CCW range from 2.5 to 3.5 times the conventional aircraft in Fig. 12. The generation of high induced drag on approach is of great benefit, as it offsets thrust and allows equilibrium flight down steeper glide slopes onto smaller runways. Figure 13 shows that approach speed reductions of 36–47% are possible when blowing is applied to the 737/CCW. The positive effect of head winds on reducing landing ground roll is seen in Fig. 14, where the full weight range of 737/CCW aircraft experience less than 500-ft ground rolls on a standard day with a 20-kt head wind. Figure 15 depicts the resulting 54–76% reductions in landing ground roll due to CCW, even with no head wind. In these data, either spoilers or shutdown of CCW blowing were applied during the ground rolls to unload the wing and add weight to the gear for better braking. Note that an alternate advantage of blowing is that a much greater aircraft gross weight can be landed by the blown aircraft in the same ground roll distance as the conventional aircraft. For instance, on a 90-deg day (Fig. 15), a 145,000-lb B737/CCW aircraft can land in the same 1270-ft ground roll required for a 65,000-lb basic B737, resulting in a 123% gross weight overload capability produced by CCW.

A related concern, of course, is whether the existing landing gear can absorb the extra weight. Figure 16 shows the predicted vertical component of kinetic energy EK_V resulting from landing at the speeds shown in Fig. 13. If the maximum B737 gross weight of 101,000 lb is taken as an upper bound on weight for the conventional aircraft at 90°F, the landing limit on vertical kinetic energy that can be absorbed at this aircraft weight is approximately 0.32×10^6 ft-lb. This value is not experienced by the B737/CCW aircraft until the weight is approximately 150,000 lb at 90°F. Thus, these large overload capabilities appear entirely feasible when considering gear loads; wing structural loads or other constraints still need to be evaluated. These types of analyses will be essential to performance prediction for advanced transports fitted with CCW, even though commercial operational requirements may vary from those applied here. These takeoff and landing performance analysis routines show relative performance im-

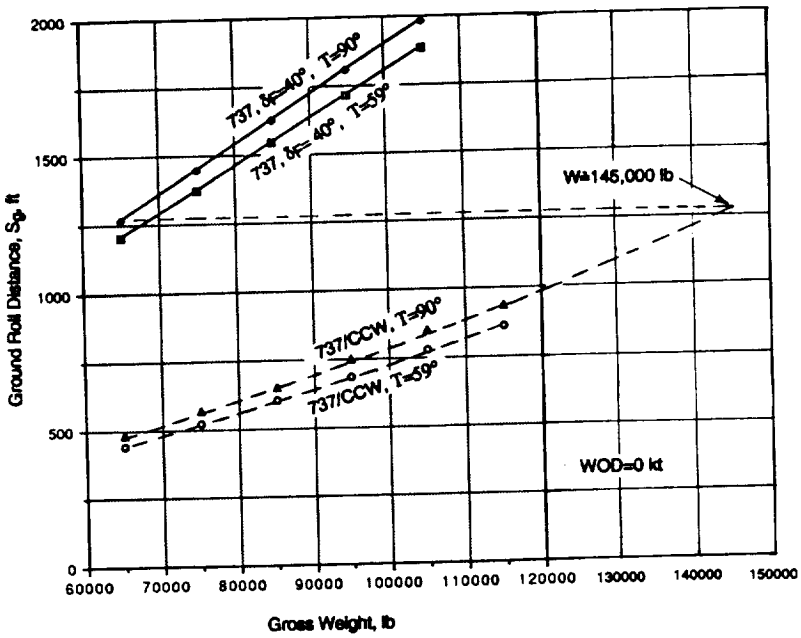

Fig. 15 Predicted landing ground roll for B737 and B737/CCW aircraft at sea level with no head wind.

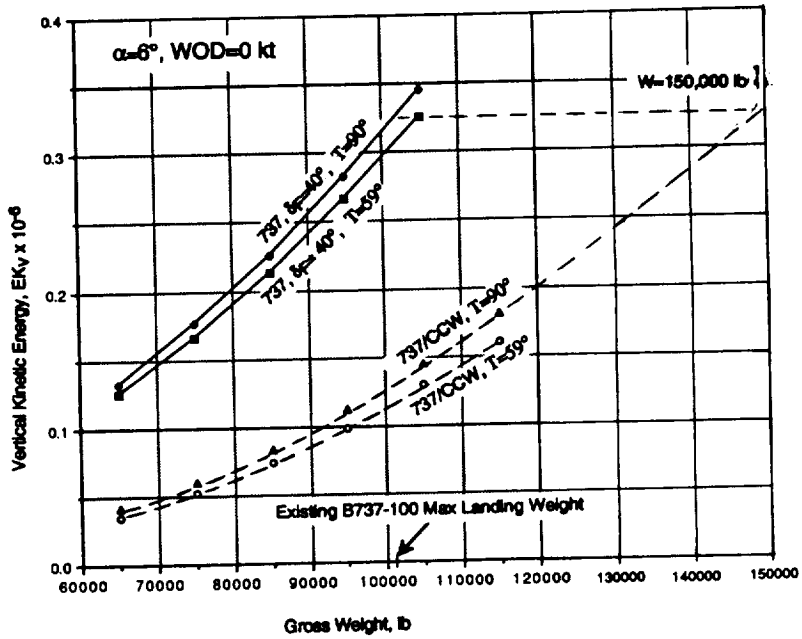

Fig. 16 Vertical kinetic energy resulting from B737 and B737/CCW landing at sea level with no head wind.

provements and should be used for further analysis once additional trimmed aerodynamic and propulsive data become available for the Boeing 737, or other representative current-day commercial subsonic transport aircraft, both with and without blowing.

Conclusions

The above three-dimensional analytical results confirm that the high-lift potential (two-dimensional C_l of 8 at $\alpha = 0$ deg) of advanced circulation control airfoils is a viable means for improving the takeoff and landing performance of representative subsonic transport aircraft. Control of overall wing characteristics (lift, drag, and moments) on these aircraft is available to the pilot through variations of blowing rates, angle of attack, leading-edge (LE) or trailing-edge (TE) flap deflections, and slot height. These results offer the potential for reduced complexity and lower terminal-area noise levels for subsonic transport aircraft equipped with CCW high-lift systems, and indicate similar payoffs for higher-speed transports. The results, together with those from Part I of this study, strongly suggest the potential of practical CCW transport configurations to provide the following capabilities:

1) CCW performance will greatly reduce takeoff and landing speeds, yielding reduced runway lengths, smaller noise footprints, and increased safety of flight in terminal areas.

2) Greatly increased liftoff gross weight and landing weight developed by smaller wing area will allow transport wings that are more optimized for cruise and greater cruise fuel efficiency.

3) Pneumatic CCW configurations will greatly reduce high-lift system complexity, as will the combination of high-lift, roll-control, and direct-lift-control surfaces into a single multipurpose pneumatic surface.

4) Steep climbout and approach flight paths due to STOL capability can yield reduced noise exposure to surrounding communities.

It is thus recommended that further development be pursued.

Acknowledgments

This project was sponsored by NASA Langley Research Center under Contract NAS1-19061. Work currently under way and just briefly reported on here is being funded under Grant NAG1-1517. The NASA Technical Monitor at Langley Research Center was Edgar G. Waggoner, Head, Subsonic Aerodynamics Branch, to whom the authors would like to express their appreciation for his continued support and encouragement.

References

[1]Englar, R. J., and Applegate, C. A., "Circulation Control—A Bibliography of DTNSRDC Research and Selected Outside References (Jan. 1969 to Dec. 1983)," David Taylor Naval Ship R&D Center (DTNSRDC), Rept. 84/052, Carderock, MD, Sept. 1984.

[2]Englar, R. J., "Experimental Investigation of the High Velocity Coanda Wall Jet Applied to Bluff Trailing Edge Circulation Control Airfoils," M.S. Thesis, Univ. of Maryland, Dept. of Aerospace Engineering, June 1973; see also Naval Ship R&D Center (NSRDC), Rept. 4708, Aero Rept. 1213, AD-A-019-417, Carderock, MD, Sept. 1975.

[3]Jones, D. G., "Measurements of Wall Jet Development on a Circulation Control Aerofoil," Univ. of California, Davis, Mechanical Engineering Dept., Davis, CA, Jan. 1971.

[4]Englar, R. J., "Two-Dimensional Subsonic Wind Tunnel Tests of Two 15-Percent-Thick Circulation Control Airfoils," Naval Ship R&D Center, NSRDC TN AL-211, AD 900-210L, Carderock, MD, Aug. 1971.

[5]Englar, R. J., "Development of the A-6/Circulation Control Wing Flight Demonstrator Configuration," David Taylor Naval Ship R&D Center, DTNSRDC Rept. ASED-79/01, Carderock, MD, Jan. 1979.

[6]Williams, R. M., and Howe, H. J., "Two-Dimensional Subsonic Wind Tunnel Tests of a 20-Percent Thick, 5-Percent Cambered Circulation Control Airfoil," Naval Ship R&D Center, NSRDC TN AL-176, AD 877-764, Carderock, MD, Aug. 1970.

[7]Englar, R. J., "Low-Speed Aerodynamic Characteristics of a Small Fixed-Trailing Edge-Circulation Control Wing Configuration Fitted to a Supercritical Airfoil," David Taylor Naval Ship R&D Center, DTNSRDC Rept. ASED-81/08, Carderock, MD, March 1981.

[8]Englar, R. J., and Huson, C. G., "Development of Advanced Circulation Control Wing High-Lift Airfoils," AIAA Paper 83-1847, July 1983; see also *Journal of Aircraft*, Vol. 21, No. 7, 1984, pp. 476–483.

[9]Wilson, M. B., and Von Kerczek, C., "An Inventory of Some Force Producers for Use in Marine Vehicle Control," David Taylor Naval Ship R&D Center Rept. DTNSRDC-79/097, Carderock, MD, Nov. 1979.

[10]Englar, R. J., Hommerly, R. A., Moore, W. H., Seredinsky, V., Valckenaere, W. G., and Jackson, J. A., "Design of the Circulation Control Wing STOL Demonstrator Aircraft," AIAA Paper 79-1842, Aug. 1979.

[11]Pugliese, A. J., and Englar, R. J., "Flight Testing the Circulation Control Wing," AIAA Paper 79-171, Aug. 1979.

[12]Englar, R. J., and Williams, R. M., "Test Techniques for High Lift Two-Dimensional Airfoils with Boundary Layer and Circulation Control for Application to Rotary Wing Aircraft," *Canadian Aeronautics and Space Journal*, Vol. 19, No. 3, pp. 93–103, 1973; see also Naval Ship R&D Center, NSRDC Rept. 4645, AD-A-015-623, Carderock, MD, July 1975.

[13]Paulson, J. W., Jr., "Wind Tunnel Results of the Aerodynamic Characteristics of a 1/8-Scale Model of a Twin-Engine Short-Haul Transport," NASA TM X-74011, April 1977.

[14]Raymer, D. P., *Aircraft Design: A Conceptual Approach*, AIAA Education Series, Washington, DC, 1989.

[15]Anon., "Specifications, U.S. Commercial Transports," *Aviation Week & Space Technology*, March 8, 1992, pp. 118, 119.

[16]Englar, R. J., Frank, L. A., and Murphy, R. D., "Preliminary Study of Candidate Aircraft for a Circulation Control Wing High Lift Flight Demonstrator," Naval Ship R&D Center, NSRDC Rept. ASED-330, AD-B004-722L, Carderock, MD, Dec. 1974.

[17]Englar, R. J., "Development of Circulation Control Technology for Powered-Lift STOL Aircraft," NASA Ames Circulation Control Workshop, Paper No. 22, Feb. 1986; see also *Proceedings of the 1986 Circulation Control Workshop*, NASA, Moffett Field, CA, 1986, pp. 491–537 (NASA CP 2432).

[18]Englar, R. J., Nichols, J. H., Harris, M. J., Eppel, J. C., and Shovlin, M. D., "Circulation Control Technology Applied to Propulsive High Lift Systems," Society of Automotive Engineers Aerospace Congress and Exposition, SAE Paper 841497, Long Beach, CA, Oct. 1984.

[19]Englar, R. J., et al., "Development of Circulation Control Technology for Application to Quiet Advanced Subsonic Transport Aircraft," Georgia Tech Research Inst., Rept. A-8612-006, Atlanta, GA, Dec. 1991.

APPLICATION OF PNEUMATIC LIFT AND CONTROL SURFACE TECHNOLOGY TO ADVANCED TRANSPORT AIRCRAFT

by

Robert J. Englar, Principal Research Engineer
Georgia Tech Research Institute
Aerospace Sciences Lab
Atlanta, Georgia 30332-0844

TRANSPORTATION BEYOND 2000:
ENGINEERING DESIGN FOR THE FUTURE

September 26-28, 1995

Comparison of Circulation Control Wing and Mechanical High-Lift Systems

The application of tangential blowing to round or near-round trailing edges of helicopter rotor blade sections has been under development and flight testing for a number of years. Very high lift augmentation, ($\Delta C_l/C_\mu$= 80-100 without any moving flap components) was verified during two-dimensional (2-D) wind-tunnel testing. This suggested the application to high-lift systems of fixed wing aircraft. As shown in the figure below, the application of a trailing edge radius equal to 0.9 % wing chord produced maximum lift coefficients nearing 7.0, and values of 6 at α=0°. The real potential is the very low blowing coefficient (C_μ= mass flux x jet velocity/qS) at which these values are achieved; these coefficients could conceivably be obtained from direct bleed of existing engines (to be discussed later). An interesting comparison between the blown airfoil and the multi-element mechanical high-lift systems is shown. It required double or triple-slotted flaps and mechanical leading edges to achieve lift performance comparable to the blown no-moving-part CCW/Supercritical section shown. The following figures show the confirmation of blown high-lift augmentation during flight test and further airfoil/wing developments as background. These lead up to recent developments of advanced pneumatic high-lift and control-surface configurations and applications.

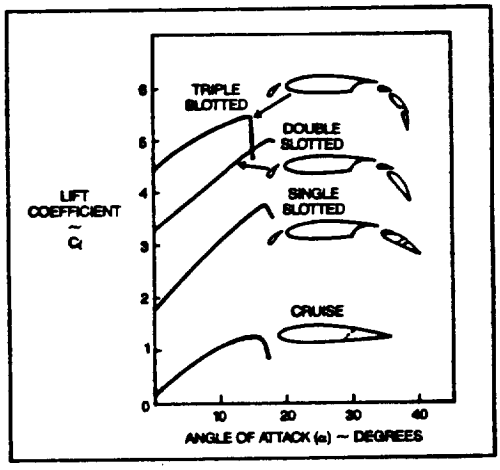

MULTI-ELEMENT MECHANICAL HIGH-LIFT AIRFOILS

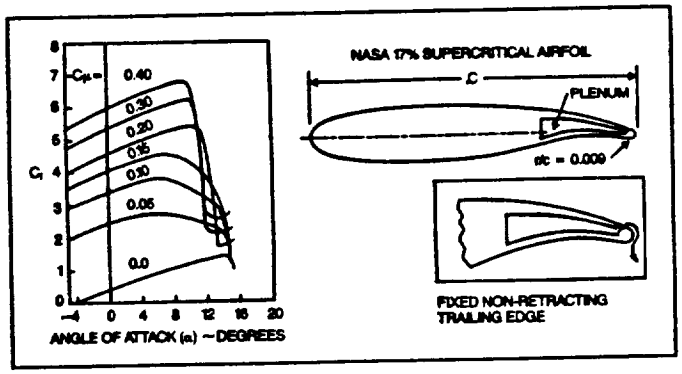

NO-MOVING-PART CCW/SUPERCRITICAL AIRFOIL

Dual-Radius Circulation Control Wing Configuration with Krueger Leading-Edge Device

The one disadvantage of the round or near-round CCW configuration was high base drag in cruise. An alternate configuration known as the Dual-Radius CCW airfoil was developed at David Taylor Naval Ship R and D Center and at Lockheed Aeronautical Systems Company-Georgia. As shown here applied to a 17% supercritical airfoil, this short-chord flap rotated up to 90° about a lower surface hinge point, exposing a small-radius (r_1) CCW surface. The upper surface of the small flap (normally 10-11% chord, but as low as 5% chord has been demonstrated) was a second much larger radius (r_2) which provided excellent jet turning when deflected to flap angles as high as 90°. When retracted, a sharp trailing edge existed for cruise, and the large upper surface radius yielded little if any aft flow separation. The airfoil shown here was tested extensively at LASC-Georgia. A mechanical Krueger leading-edge flap deflected 60° was initially installed to keep the leading edge flow attached at the very large supercirculation and high upwash produced by the blown trailing edge. Results are shown on the following pages.

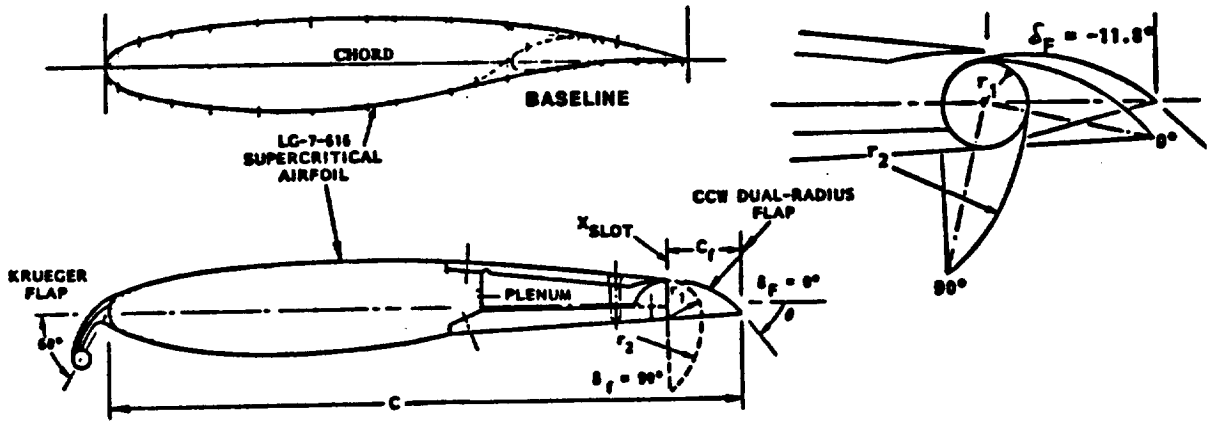

2-D CCW Lift Comparison Showing 3-D and Tip Vortex Effects

These data show lift performance at α=0° for both the 2-D dual-radius-CCW airfoil with a 60° Krueger LE flap and 90° CCW flap and an aspect-ratio 5.5 semi-span wing created when this airfoil model was retracted through the tunnel floor. Two-dimensional lift values of nearly 8 were generated for C_μ of 0.4. The lift improvement of this dual-radius flap over the previous round CCW trailing edge is approximately 35% and is accompanied by greatly reduced cruise drag (to be discussed later). The 2-D lift improvement represents a factor of 2 to 4 increase over the mechanical flaps of previous slides at α=0°. Note also the lift reductions that occur due to tip vorticity and span wise effects when the airfoil is converted to a 3-D semi-span wing. Nevertheless, the resulting C_L values of greater than 5 at α=0° are still appreciable.

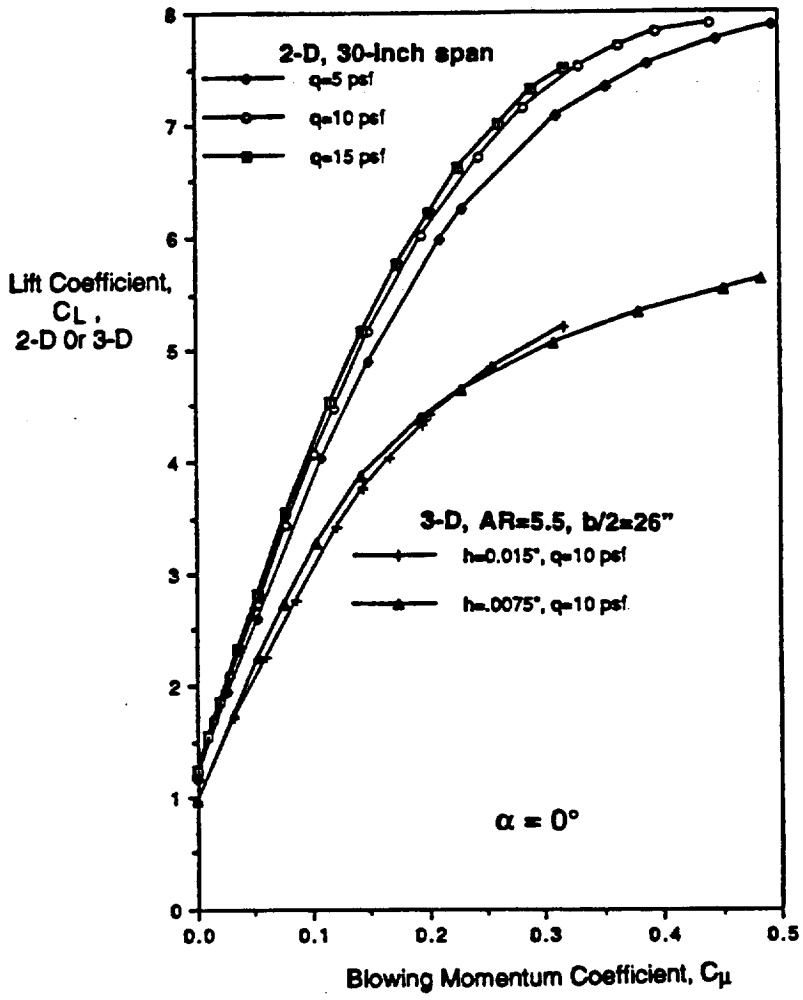

Blown Leading Edge Lift and Stall Improvements

Blown airfoil lift curves are shown below to compare the Krueger flap mechanical leading edge (identified as K) with the blown leading edge (LE) of the previous page. For reference, the clean cruise airfoil is also shown. Note here the Krueger lower surface stall at C_μ=0, and that for any constant value of trailing edge C_μ, the LE blowing shows significantly higher stall angle, as well as, greater lift at lesser incidence. This is because, unlike mechanical LE devices at low incidence the LE blowing itself adds to the supercirculation of the airfoil. Leading edge blowing alone was found to traverse all the way to the trailing edge dual-radius flap and remain attached to at least a portion of the flap arc, thus augmenting lift. Thus, a non-moving pneumatic LE and a short-chord dual-radius CCW trailing edge yielded very high lift augmentation even at α=0°.

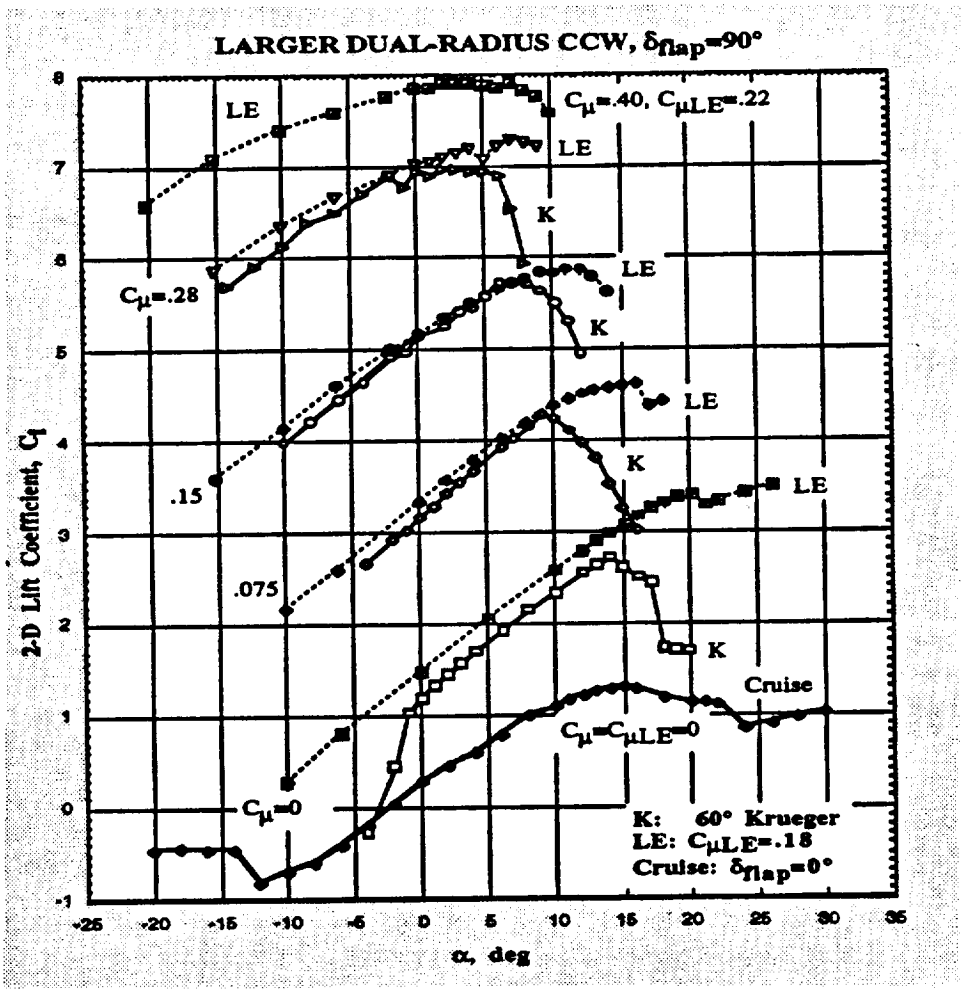

Predicted Boeing 737 and 737/CCW Takeoff and Approach Speeds

Terminal area speeds of the conventional 737 are a function of gross weight, flap angle and temperature, as shown below. Corresponding 737/CCW speeds vary with available blowing instead of flap angle which is fixed here at 90°. Available blowing corresponds to bleed of existing fan bypass air. Blowing reduces liftoff speeds by between 15 and 40%, depending on aircraft weight and temperature. Approach speeds were decreased by 36 to 47% by blowing. One imagines that these could be even greater reductions if more air were available, say from an onboard APU dedicated to high lift in terminal area operations, but to heating, air conditioning and/or pressurization at other times.

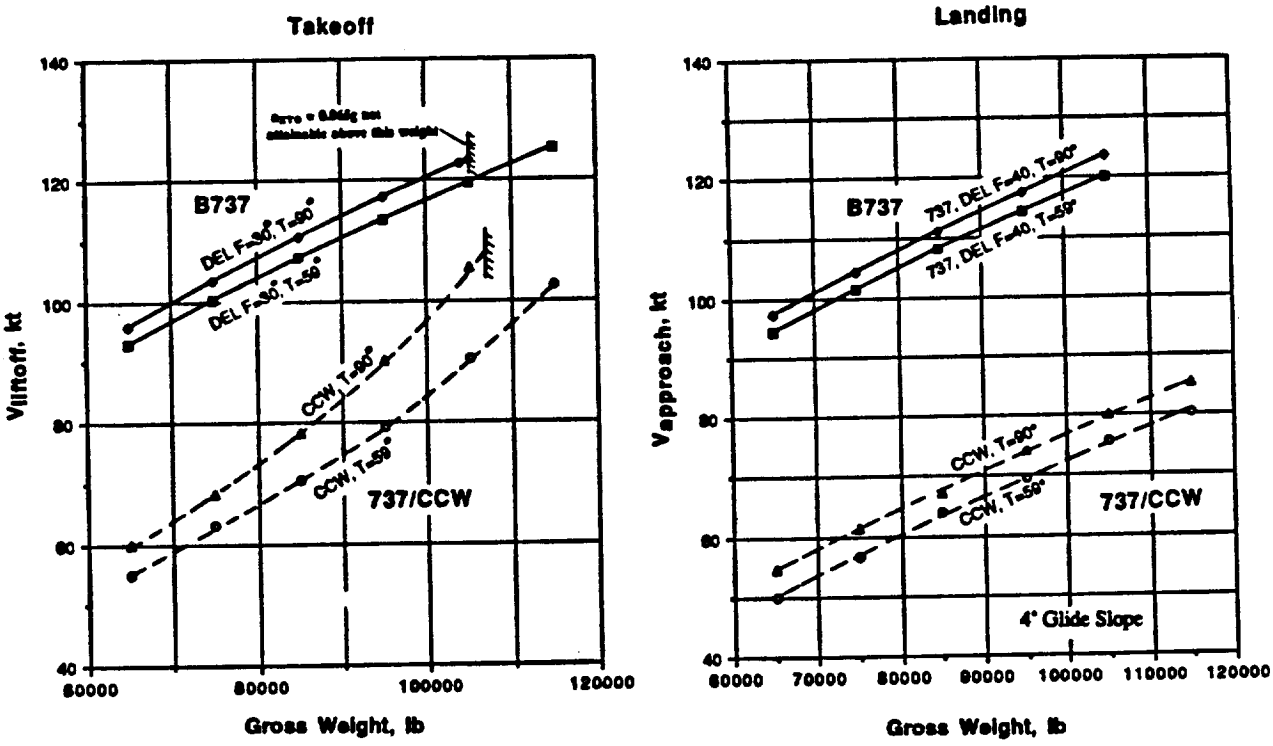

Predicted 737 and 737/CCW Takeoff Ground Rolls at Sea Level

This data applies to previously mentioned takeoff speeds, available with and without blowing, and includes thrust loss due to bleed where appropriate. Blowing has been reduced where necessary to assure that a minimal acceleration at liftoff of 0.065g was available, a Navy one-engine-out restriction. Ground roll reductions from 37 to 80% result, with the greatest reductions being at lighter weights. Again, increases in gross weight that could be lifted airborne at a constant ground roll distance show very large improvements for the blown aircraft over the conventional configuration.

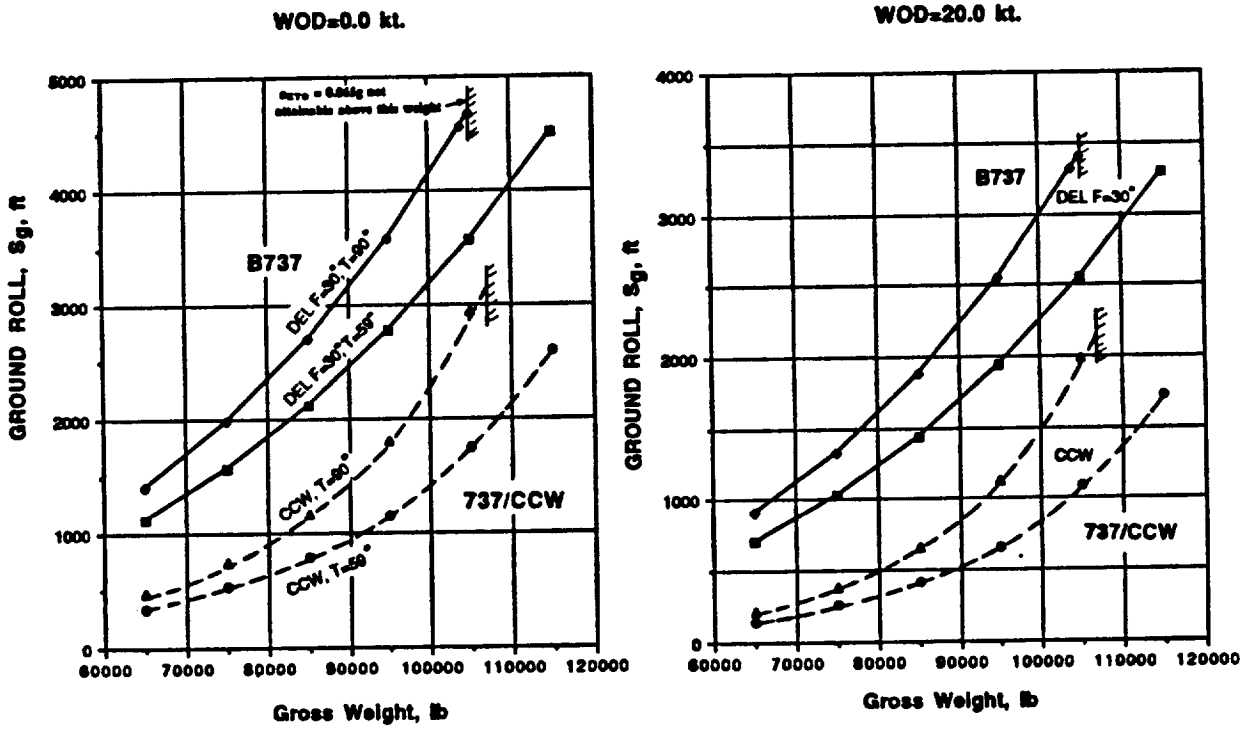

Short Field Capability for Pneumatic Commercial Aircraft (??)

Thanks are due to Southwest Airlines Company for this interesting picture which we downloaded from their World Wide Web home page. The previous data indicates that these ground roll distances, implied in jest here by the airline, are already possible for a light weight 737-CCW commercial aircraft. Given optimization of the flap angle and addition of leading edge blowing, ground rolls of these short distances should be possible for a much larger range of weights for pneumatic commercial airliners.

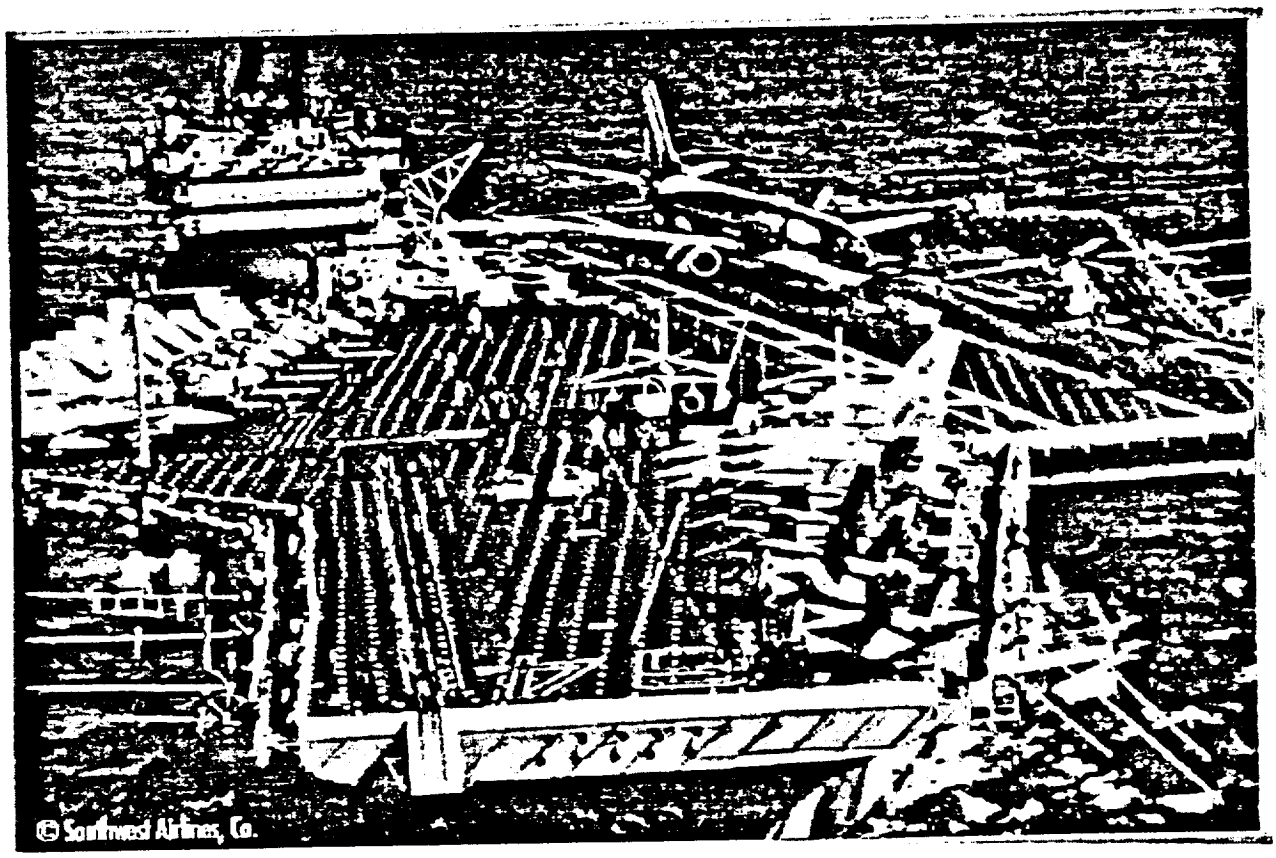

Advanced Dual-Radius CCW/Supercritical 2-D Airfoils

The ultimate goal in the development of pneumatic airfoils is to design one with very high-lift capabilities, no cruise drag penalty, few or no moving parts, and minimal changes to the baseline cruise airfoil configuration. The dual-radius CCW configuration with leading edge blowing as previously discussed was close to this goal. However, to ensure excellent CCW jet turning, an enlarged trailing edge radius had been chosen which exceeded the original supercritical airfoil contour. A more recent configuration is shown below, the small dual-radius CCW airfoil. Here the initial radius (R_1) has been cut in half relative to the previous airfoil so that the undeflected flap falls within the cruise airfoil contour. This produces an initial radius of 3% wing chord and a flap chord of less than 10% wing chord. Again, leading-edge blowing is employed. The same CCW airfoil as previously tested has been modified into this configuration. The following slides will present representative data. It should be noted that the plenums shown are probably oversized relative to actual aircraft application. Here they had to contain pressure recording equipment and static pressure tubing while still not distorting plenum flow.

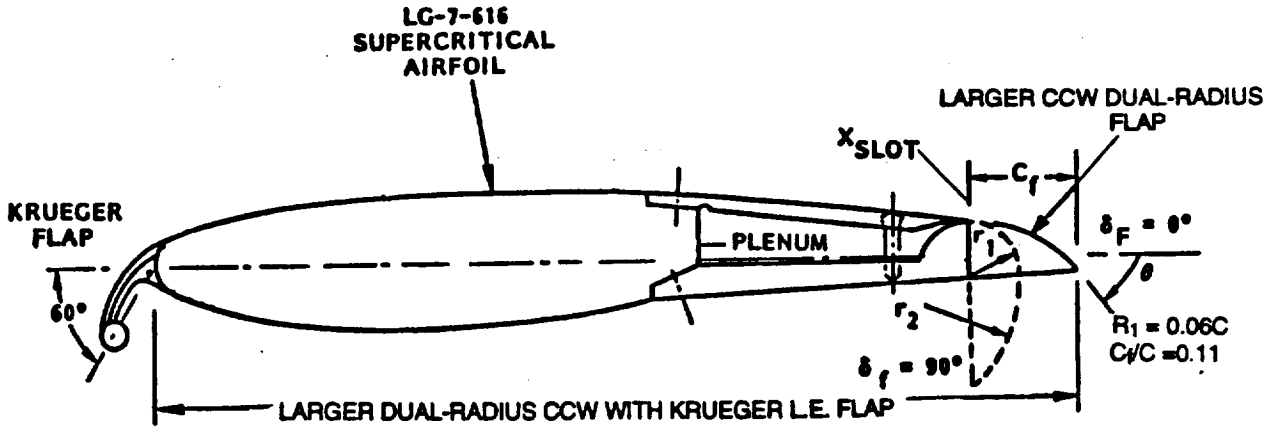

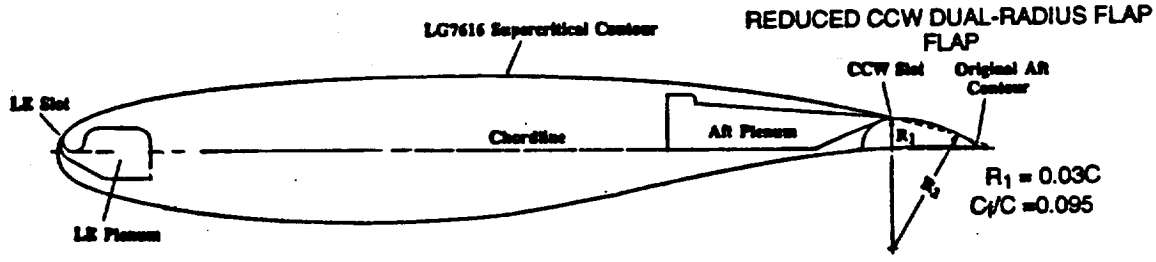

SMALL DUAL-RADIUS CCW WITH L.E. BLOWING

Force Amplification of Small Dual-Radius CCW Airfoil $\delta_{flap}=0°$

At this point, only the undeflected-flap configuration has been evaluated in the tunnel with blowing, but the results are quite enlightening since this represents the cruise airfoil. For reference in the data below, we have included the recent NASA Energy Efficient Transport (EET) airfoil, from AIAA Paper 95-1858. This is a single-slotted flap/slat high-lift airfoil, where the less complex single-slotted flap is used to reduce parts count, complexity, cost, and noise due to turbulence over multi-element flaps. Its cruise airfoil is a 12% thick supercritical airfoil and test Reynolds number ran from 9 to 16 million. The current CCW airfoil is a 17% thick supercritical design with high-lift test Reynolds number less than one million. The results below show that the smaller CCW flap performed better than the larger CCW configuration, probably because of the increased aft camber of the supercritical airfoil. Note that this new airfoil with no moving parts can produce lift coefficients of nearly 6. That compares favorably with the NASA EET airfoil, which, by necessity, is subject to considerable high-lift system optimization, including flap and slat angle, gap, overhang, Reynolds number, etc. Observe the considerable loss in lift performance and drag increase which result when the flap overhang varies slightly from the optimized value (OH=-0.0025c). The unblown minimum cruise drag of the CCW airfoil falls in the very acceptable range of around 0.0112-0.0113. (The corresponding cruise drag for the larger dual-radius CCW airfoil at the same conditions was 0.0156-0.0160). The addition of blowing to the cruise airfoil reduces the measured drag to negative values. The negative drag increment produced is on the same order of magnitude as the C_μ applied; that is, there is high thrust recovery from the blown surfaces. The implication here is that airfoil efficiency (l/d) can be very high and can be adjusted during flight by variation in blowing. The fact that this no-moving-part blown airfoil generates greater lift from blowing values on the order of C_μ =0.1 than the flapped and slatted mechanical airfoil, speaks very highly for this new configuration. It also suggests the possibility of no-moving part blown surfaces to replace aileron, spoiler, rudder, and elevator control surfaces on conventional aircraft.

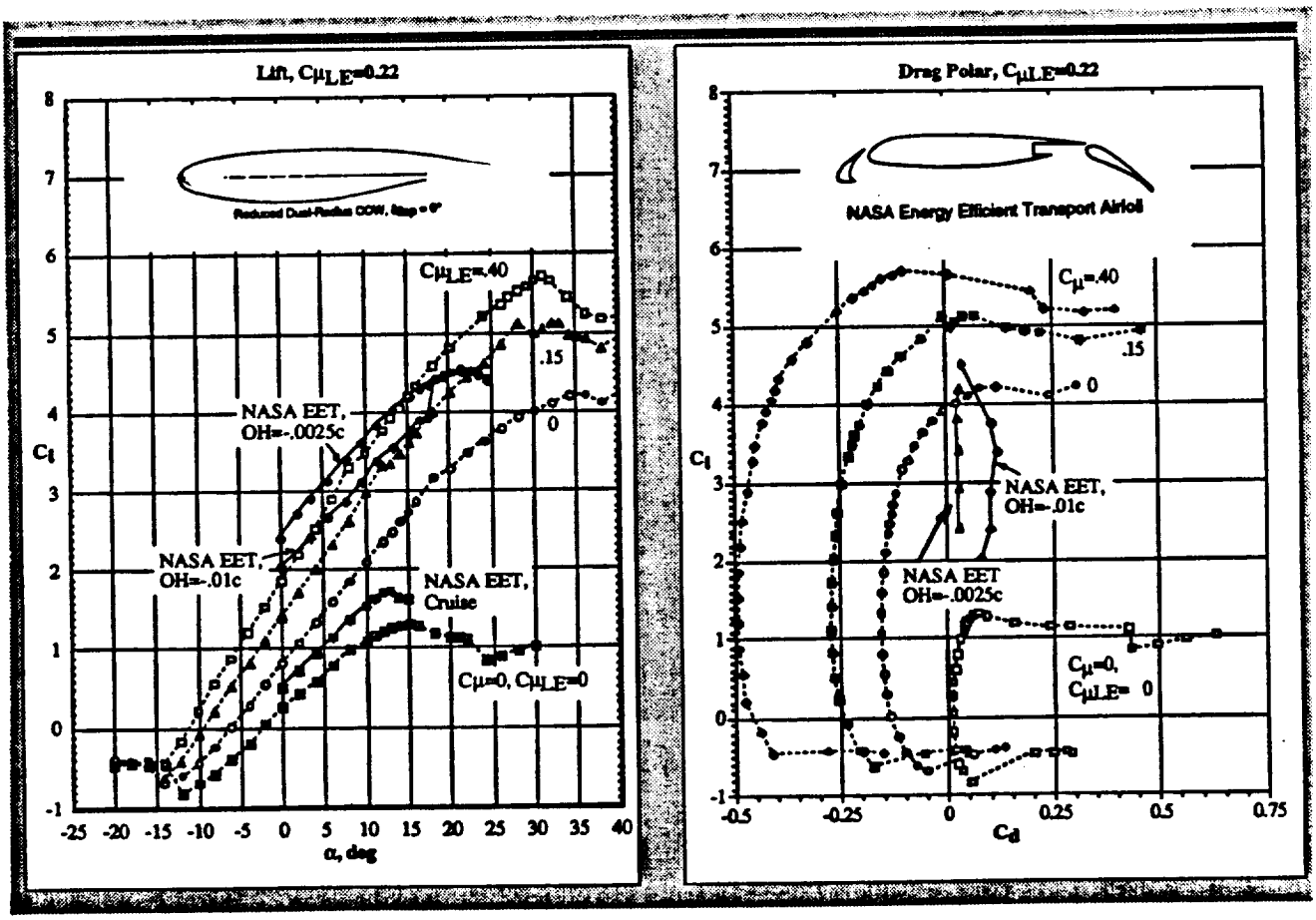

Blown Canard on Generic High Speed Civil Transport Model

Pneumatic technology is not limited to advanced subsonic transport aircraft. Current designs for proposed High Speed Civil Transport configurations employ highly swept wing designs and achieve high lift augmentation by leading edge vortex generation. This, however, usually requires approach and takeoff at very high angles of attack. This has required additional tail power and such unusual features as nose droop on some designs. Recently, GTRI has investigated for NASA the application of pneumatic technology to HSCT configurations to provide alternative means of lift and angle of attack control. Blown circular-cylinder canards had been applied to National Aerospace Plane configurations to provide pitch control for takeoff, and strong control of wing vortex burst had been discovered to result as well. The same concept was applied here to a generic HSCT configuration. Two blown canards were applied to a half-span NASP model which had a wing planform very similar to HSCT planforms. These canards included Canard 1 (AR=1.3 with forward-swept trailing edge) and Canard 3 (AR=2.6, with aft-swept trailing edge) as shown below. Each of these canards had an aft-blowing slot and a dual-radius-type trailing edge flap. This flap was deflectable, but all of the data shown here were obtained with 0° deflection. The picture shows the higher-aspect-ratio canard with blowing mapped by a tuft. Flow visualization showed that when blowing was applied, the downwash behind the canard delayed vortex burst on the wing because of reduced upwash over the wing leading edge.

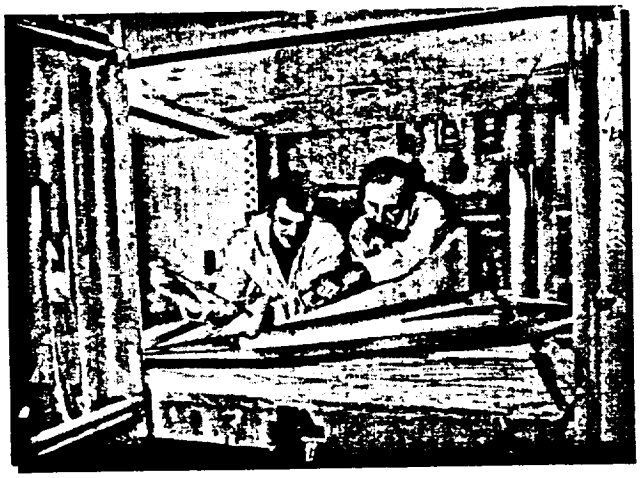

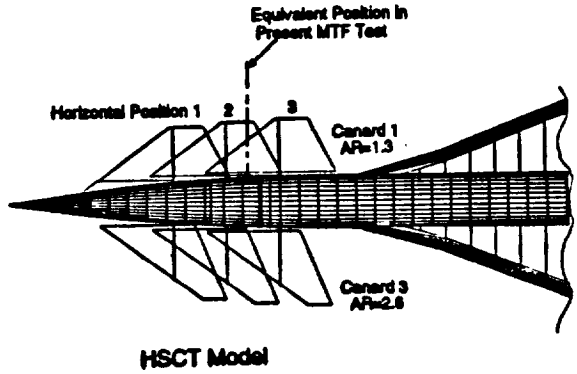

Blown Canard Planforms

Cyclic Blowing and Load Tailoring

Additional opportunities exists for pneumatic lift and control of both low-speed and high-speed transports. It has been shown during earlier pneumatic applications to helicopters that pneumatic blowing could be made to vary quite rapidly (30 cycles per second or more). Recent applications to fixed-wing aircraft show additional benefits. From a control standpoint, aerodynamic response at 30 cycles per second is quite beneficial. We have also found that cyclic blowing can reduce the amount of mass flow required from the engine to augment aerodynamic forces. For instance, a time-averaged lift can be obtained at an average mass flow which is less than the constant mass flow value required for the same lift under steady-state conditions. From a controls standpoint, it is also possible to pneumatically tailor both the spanwise lift loading (and thus the induced drag) as well as the lifting surface root bending moments. It is possible to provide an elliptic spanwise slot distribution and thus an elliptic lift distribution with the associated minimum induced drag. It is also possible to reduce tip loadings due to gusts by adjustment of blowing values near the wing tip.

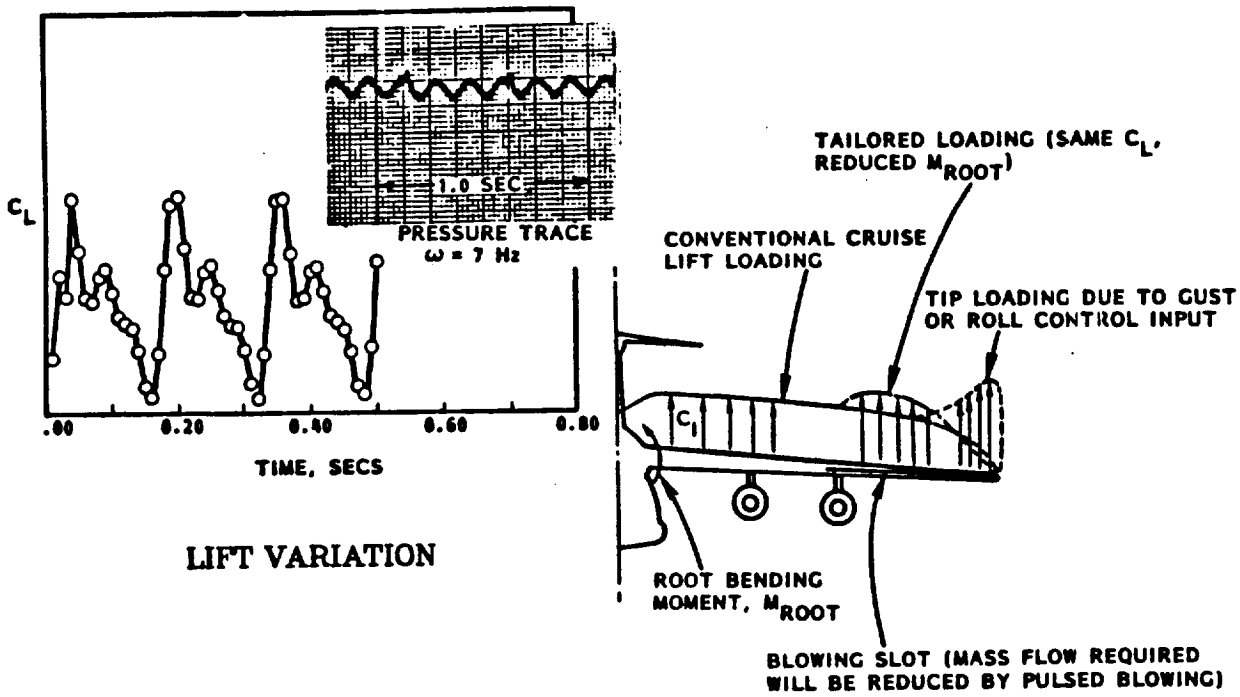

Challenge to American Aerospace Technology

The American commercial aircraft industry is under challenge from foreign competitors in terms of both Advanced Subsonic Transports (AST) and the High Speed Civil Transport (HSCT). For example, during its first commercial flight in June 1995, the latest Boeing airliner, the 777, was already competing against two similar foreign aircraft, the A330 and A340 (by the European consortium Airbus Industrie including member companies from Britain, France, Germany and Spain). The American MD-11 aircraft faces similar competition. US airlines are already buying and flying a number of these foreign-built aircraft (see below). American industry has yet to produce even a prototype HSCT, but the British/French consortium built the Concorde supersonic transport which has been flying commercially (with flights into the US) since 1976. ***American advanced transport technology is behind.*** Even though numerous research programs have been conducted over the years and promising technology developed, a concentrated efficient integration of these technologies (including thorough environmental and economic impact analyses) has not been completed. The next generation of efficient commercial aircraft must exhibit superior performance; satisfy all noise and environmental requirements; and exhibit adequate economic potential by satisfying the interests of airlines and by offering an affordable ticket price to the passenger. In order to achieve all these objectives, the designer must, early in the design process, account for cost of operation and reliability/maintainability. **State-of-the-art aerodynamic, propulsive, control, noise, and operational technologies need to be developed, and a logical means to effectively integrate these into promising advanced US designs needs to be employed. Advances in pneumatic technology and its application to American transport designs can yield major benefits to our industry.**

ValuJet nearing purchase of new jets

Airbus A319 is insider favorite (Atlanta Journal-Constitution, 9/20/95)

By [redacted]
Staff writer

Northwest Airlines Airbus A320

What's Needed??

Proof of concept verification of much of this pneumatic technology has already occurred, and patents exist or have been applied for. Immediate research and systems analysis that need to be accomplished near-term are shown below. Applications to near-term designs such as the Advanced Subsonic Transport and the High Speed Civil Transport should take precedence. Integration of aerodynamic, propulsion, stability & control, and acoustics teams into a unified design effort is essential.

WHAT'S NEEDED??

- High Speed Performance of Pneumatic Airfoils
- Mission Integration; System Analysis; Payoffs & Penalties; MDO
- Experimental /CFD Evaluation for Particular Configurations/Applications
- Full-Scale Proof-of-Concept on Subsonic Commercial Transport
  Has Already Been Proof-of-Concept Flight-Tested on Military Aircraft
- Operations Analysis, New Uses:
  - Noise Abatement
  - Wing Downsize
  - Systems Synergistic Integration
- HSCT - Configuration Optimization

AIAA 97-0036

Pneumatic Lift and Control Surface Technology Applied To High Speed Civil Transport Configurations

Robert J. Englar, Curt S. Niebur, and Scott D. Gregory

Aerospace & Transportation Laboratory
Georgia Tech Research Institute
Georgia Institute of Technology
Atlanta, GA 30332-0844

35th Aerospace Sciences Meeting & Exhibit

January 6-10, 1997 / Reno, NV

AIAA 97-0036

PNEUMATIC LIFT AND CONTROL SURFACE TECHNOLOGY APPLIED TO HIGH SPEED CIVIL TRANSPORT CONFIGURATIONS

Robert J. Englar*, Curt S. Niebur**, and Scott D. Gregory**
Aerospace & Transportation Laboratory
Georgia Tech Research Institute
Atlanta, GA 30332-0844

ABSTRACT

Experimental evaluations have been conducted of blown high-lift devices and control surfaces applied to improve the low-speed performance of generic High Speed Civil Transport aircraft. Plain blown flaps and advanced pneumatic high-lift devices have been integrated into highly-swept vortex-dominated wings. These produced large lift increases and significant drag reductions greater than full jet thrust recovery. Because conventional horizontal tails were found inadequate to trim these configurations, blown canards were employed. In addition to providing positive lift increments for trim, the canards were found to favorably influence the higher angle-of-attack vortex-lift characteristics of these wings. The downwash from these canards resulted in delay of wing vortex burst. The paper presents details of these investigations and test results which confirm the effectiveness of combined pneumatic high-lift devices and control surfaces on these HSCT aircraft.

INTRODUCTION

Various forms of blown aerodynamic devices have been evaluated in recent years to augment the low-speed, high-lift characteristics of modern-day aircraft. These aircraft, especially military configurations, usually have relatively high wing loadings and associated high takeoff and landing speeds with long ground rolls. Use of pneumatic devices, such as blown flaps or jet flaps, can augment the lift of mechanical flaps and reduce terminal-area speeds and distances (ground roll as well as climb-out and approach flight paths). More recently, a concept known as Circulation Control (CC), which employs tangential blowing over highly rounded small trailing edges, has been shown to greatly augment lift and thus improve takeoff and landing capabilities[1-7]. For the two-dimensional airfoils of subsonic aircraft using this technology[2,4], lift augmentation of nearly 80 times the input blowing momentum has been recorded, as has significant drag reduction due to jet thrust recovery and prevention of flow separation.

Recent interest in high-speed commercial aircraft such as the High Speed Civil Transport (HSCT) suggests that this pneumatic technology should greatly benefit these vehicles as well[5]. In addition to high wing loadings, these aircraft also frequently employ vortex lift on takeoffs and landings at high angles of attack. This has required such "features" as mechanical nose droop for visibility and highly-upswept aft fuselage contours for ground clearance upon rotation. Reduced wing sweep and increased wing planform area can improve low-speed flight, but may hinder high-speed cruise performance. A recent research program conducted at Georgia Tech Research Institute (GTRI) under the sponsorship of NASA Langley Research Center has evaluated the potential of blown aerodynamic devices for both lifting surface and control surface applications to high-speed commercial aircraft. Major goals of this program were to: (1) develop advanced pneumatic high-lift configurations for highly-swept wings; (2) evaluate blown canards for pitch trim, vortex control and lift augmentation; and (3) evaluate

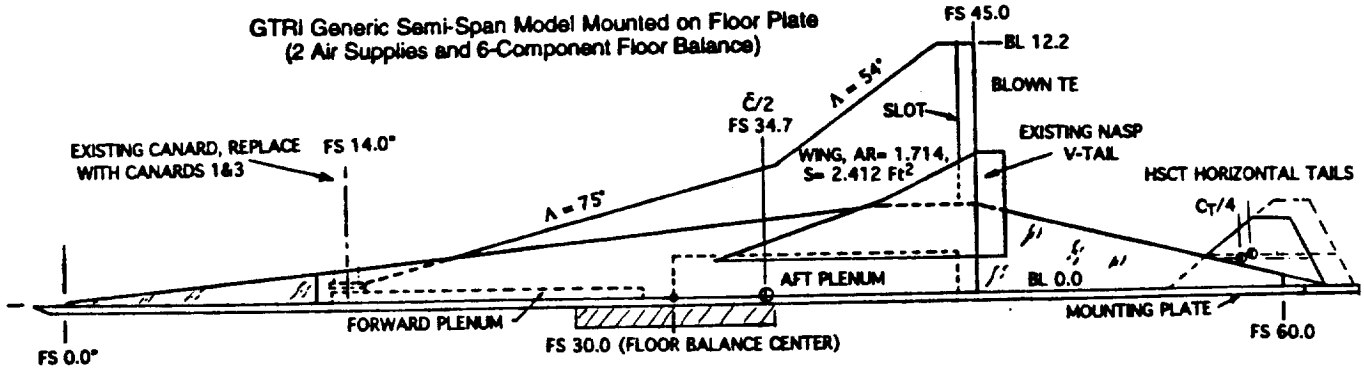

Figure 1 - Planform of the GTRI semi-span NASP/ HSCT configuration

* Principal Research Engineer; Associate Fellow, AIAA
** Cooperative Education Student; Member AIAA

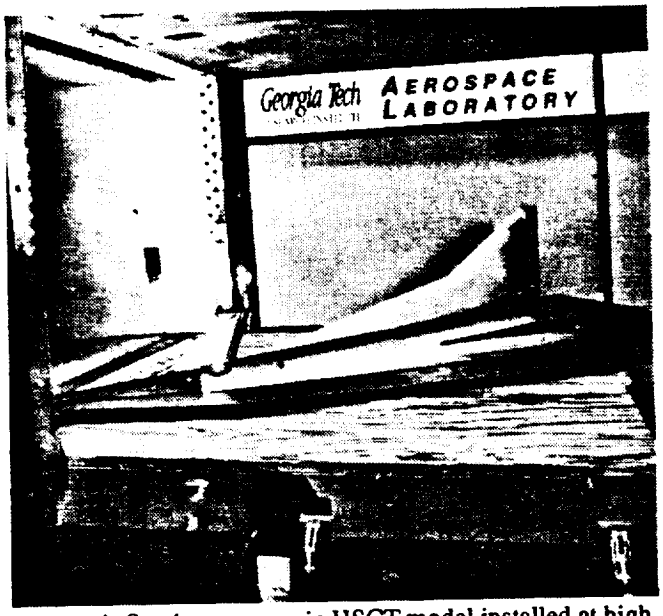

Figure 4- Semi-span generic HSCT model installed at high α in the GTRI Model Test Facility, including Canard 3

Figure 5 - Static flow visualization of blowing over 20-degree plain flap

controlled air supply lines passing through separate flow meters and through trapezes to minimize air pressure tares on the balance.

Static flow visualization (wind off) showed that the wing trailing-edge blowing jet sheet adhered to the plain flap surface and deflected 30-35° when the flap was mechanically deflected to 20° (Figure 5). In comparison, the highly curved CC trailing edge of the blown canard yielded jet turning of nearly 90° (Figure 6). Similar results were seen on the wing's CC flap configurations. Whereas this turning would prove effective in augmenting the canard's lift and providing pitch capability plus a positive lift increment to trim, the real payoff of the blown canard was expected to come from its ability to greatly reduce the upwash flowfield onto the swept wing leading edge.

Figure 6 - Static flow visualization of blowing over Canard 3 aft-swept CC trailing edge

TEST RESULTS

This generic blown HSCT model was tested subsonically over a large angle-of-attack range with each canard, with each tail, and for several flap configurations on the wing and canard trailing edges. The sketch in Figure 2 shows the canard locations relative to the wing leading edge. (Of course, on this half-span model, only one canard was tested at a time). Measured forces and moments at 0.50 MAC were corrected for small pressure tares and for the interference effects of the splitter plate. In these data, the blowing coefficients for either the wing or the canard are defined as:

$$C_\mu = \dot{m}\, V_j/(qS)$$

Here, $\dot{m}$ is the measured slot mass flow, V_j is blowing jet velocity, q is freestream dynamic pressure and S is half-wing reference planform area. (For this semi-span model, a reference area for only one wing and aerodynamic forces and moments half those of a full-span configuration yield full-span 3-D coefficients).

Canard and Blowing Effects

Canards 1 and 3 (AR = 1.29 and 2.58, respectively) were evaluated at two vertical locations: high (fuselage centerline) and low (wing plane), but only with the 20° plain flap on the wing, not with the CC flap installed. Figures 7 and 8 present the tail-off lift curves and drag polars for the baseline unblown aircraft (cruise and 20° flap), and for the 20° blown flap, both with and without the canards. From the data taken, the lower aspect-ratio Canard 1 was found to be the more effective of the two, probably because its

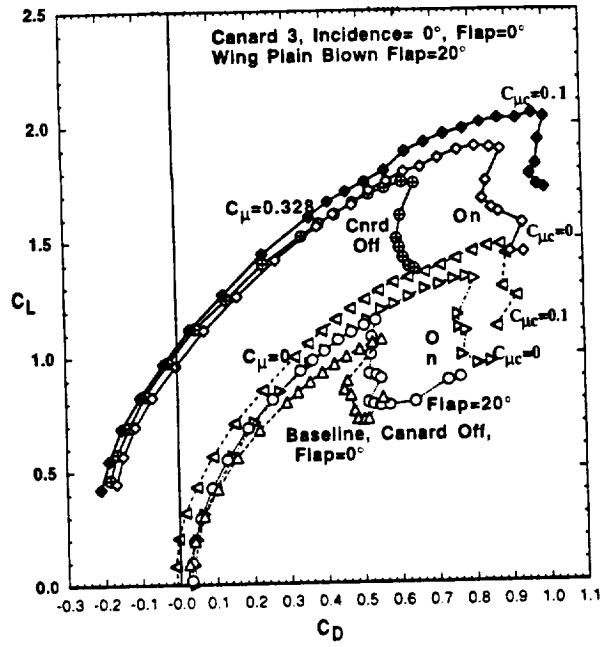

Figure 8 - Continued: **b.** Drag polars

C_μ, dF=20°	Canard 1	Position	$C_{\mu c}$	ΔC_D at C_L=1.0	C_{LMAX} Increase	α_{max} Increase
0	Off		0	-17.4%	8.5%	-6.3%
"	On	HI	"	-9.1%	32.6%	26.7%
"	"	HI	0.1	-27.8%	52.8%	32.1%
"	On+Flap	HI	0	-6.5%	37.7%	32.9%
"	"	LO	"	-4.4%	31.1%	22.9%
"	"	HI	0.1	4.4%	50.9%	45.8%
"	"	LO	"	8.7%	32.1%	43.8%
0.328	Off		0	-103.3%	65.1%	-3.8%
"	On	HI	"	-93.5%	84.0%	21.3%
"	"	HI	0.1	-106.1%	102.8%	25.8%
"	On+Flap	HI	0	-87.4%	87.7%	25.0%
"	"	LO	"	-87.0%	84.9%	17.1%
"	"	HI	0.1	-87.4%	96.2%	34.2%
"	"	LO	"	-87.0%	79.3%	45.8%

Table I- Increments due to blown Canard 1 relative to Baseline Configuration (canard off, flap=0, C_μ=0)

C_μ, dF=20°	Canard 3	Position	$C_{\mu c}$	ΔC_D at C_L=1.0	C_{LMAX} Increase	α_{max} Increase
0	Off		0	-17.4%	9.5%	-7.5%
"	On	HI	"	-17.4%	24.5%	18.3%
"	"	LO	"	- 9.1%	25.5%	-4.2%
"	"	HI	0.1	-28.3%	40.6%	28.6%
"	"	LO	"	-22.2%	40.6%	22.9%
"	On+Flap	HI	0	- 8.7%	31.1%	22.4%
"	"	LO	"	- 4.8%	26.4%	16.7%
"	"	HI	0.1	-13.0%	44.3%	28.6%
"	"	LO	"	- 4.6%	34.9%	31.3%
0.328	Off		0	-103.3%	65.1%	-1.7%
"	On	HI	"	- 95.9%	77.4%	16.2%
"	"	LO	"	- 91.3%	82.1%	20.8%
"	"	HI	0.1	-104.4%	93.4%	20.3%
"	"	LO	"	-101.1%	91.5%	21.7%
"	On+Flap	HI	0	- 91.3%	84.9%	20.3%
"	"	LO	"	- 90.9%	83.0%	12.5%
"	"	HI	0.1	- 91.3%	95.3%	20.3%
"	"	LO	"	- 84.8%	93.4%	25.0%

Table II- Increments due to blown Canard 3 relative to Baseline Configuration (canard off, flap=0, C_μ=0)

Figure 9 - Flow visualization showing vortex formation before and after canard blowing, α=29°
a. No canard blowing, vortex burst on wing

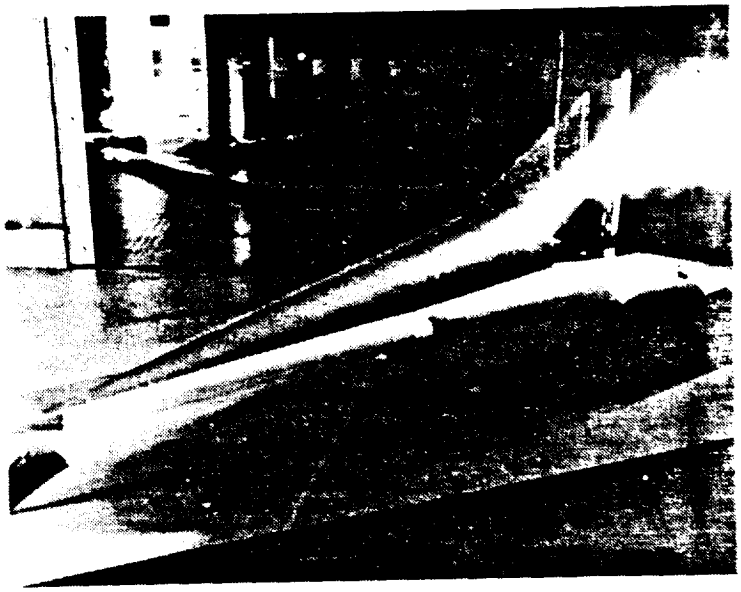

Figure 9 - (Continued)
b. Canard blowing, unburst vortex on wing

The main gain from the canard is confirmed by the vortex characteristics shown in Figure 9. This wind-on flow visualization showed that when canard blowing was applied, the strong downwash behind the canard greatly delayed or prevented vortex burst on the wing because of the reduced upwash over the swept leading edge. The first photo shows large vortex burst formation on much of the wing without canard blowing at α = 29°, which is beyond the stall angle. In the second photo, the unburst vortex is restored and the stall angle is extended by addition of the canard blowing. Figure 10 compares the lift performance of the blown canards (with flaps deflected) at different vertical locations .

One additional capability of the blown canard is

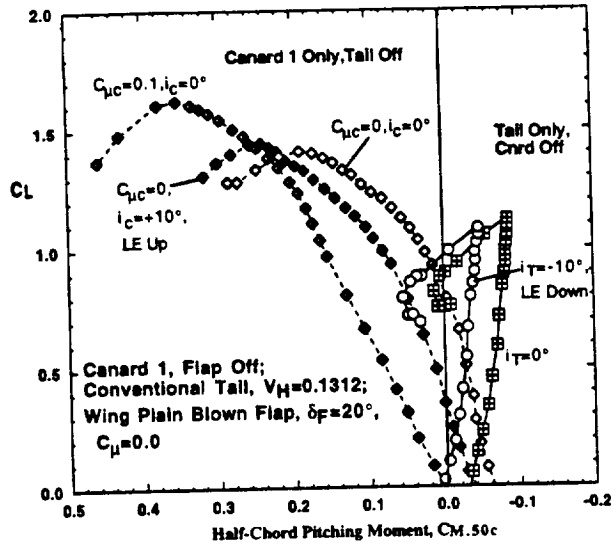

Figure 14 - Comparison of pitch trim and lift provided by horizontal tails and by blown Canard 1: a. Half-chord C_M

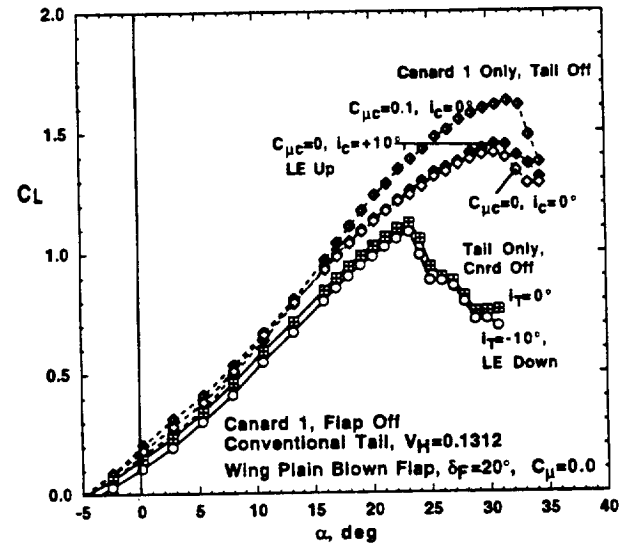

Figure 14 - (Continued) : b. Lift curves

combination of a smaller blown canard, a small horizontal tail, or further aft c.g. are suggested. Figure 14b shows the corresponding lift values.

Circulation Control Wing

Evaluation of an advanced blown wing was undertaken as a third phase of this test program. Based on the very high lift augmentation already confirmed for rounded trailing edge CCW configurations[1,2,3,4,5] but designed to keep cruise drag low, the CCW flapped configuration of Figure 3 was applied to the HSCT model. In its cruise mode, the trailing-edge circular arc provided 48° of surface arc deflection; if that arc was extended by deflection of the lower surface by about 34°, (i.e., δ_{Flap} = 34°), then the jet turning angle would be 90°. This additional flap deflection is intended to provide much greater lift augmentation as well as drag generation for use on approach.

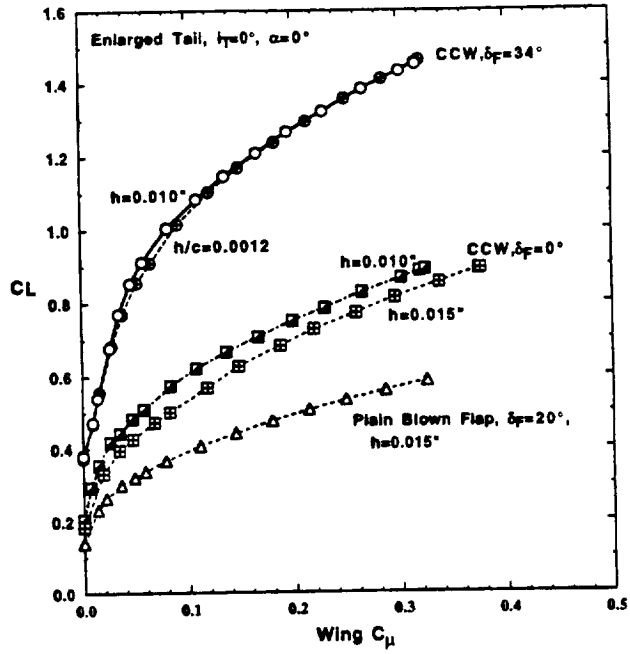

Figure 15 - Lift augmentation due to various blown TE flaps, α=0°, enlarged tail

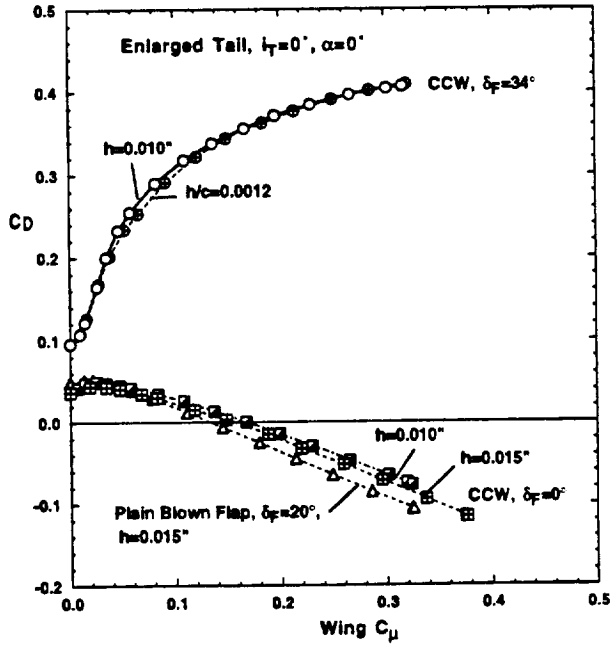

Figure 16 -Drag variation due to various blown TE flaps, α=0°, enlarged tail

Figure 15 shows how the additional jet turning of the three pneumatic flap configurations augments lift at α = 0°. The flapped CCW nearly doubles the lift of the undeflected CCW due to the additional jet turning, and nearly triples the lift of the plain blown flap. The effect of slot height variation is also seen here. Nose-down pitching moment was seen to increase with lift due to the increased aft loading produced by blowing. The ability of these three blown configurations to alter drag is shown in Figure 16, where the additional jet turning and lift also add to the induced drag. The cruise

on these highly swept wings show a 1200% return on the blowing momentum input.

- Drag reductions greater than 100%, partly due to jet thrust recovery and partly due to operation at much lower body and wing incidence to achieve a desired lift

- Lift generation at much lower angle of attack, reducing the need for such typical HSCT characteristics as drooped nose and aft fuselage upsweep.

- Blown canards (or even unblown canards) appear able to trim the nose-down pitch of these configurations, as well as to limit the circulation-induced upwash and thus delay stall due to vortex bursting

Additional trends observed were:

- Neither the conventional nor the enlarged all-flying horizontal tails were able to trim this generic HSCT configuration in the high-lift modes tested. Unless canards were added, only the unblown 20° plain flap was trimmable by the tails. The canards alone provided the necessary trim capability, but were longitudinally unstable.

- Aerodynamic lift for the wing/tail combination appeared to reach a vortex-burst-induced limiting value for this aircraft, independent of how the wing circulation was achieved (incidence, blowing, flaps, etc.). Canards can help the configuration to exceed this limit by reducing upwash onto the wing and delaying vortex burst.

It thus appears that pneumatic high-lift devices and control surfaces can offer significant improvements in the low-speed characteristics of HSCT-type aircraft. However, vortex burst and stall need to be controlled, and some form of leading-edge device or canard should be considered. Conventional tail surfaces alone do not appear adequate to trim the high-lift devices evaluated, and thus a blown canard integrated with or replacing this tail looks quite promising.

REFERENCES

1. Englar, Robert J., Marilyn J. Smith, Sean M. Kelley and Richard C. Rover III, "Application of Circulation Control Technology to Advanced Subsonic Transport Aircraft, Part I: Airfoil Development," AIAA Paper No. 93-0644; *AIAA Journal of Aircraft*, Vol. 31, No. 5, Sept-Oct. 1994, pp. 1160-1168.

2. Englar, R. J. and C. G. Huson, "Development of Advanced Circulation Control Wing High-Lift Airfoils," AIAA Paper 83-1847, 13-15 July 1983; AIAA *Journal of Aircraft*, July 1984, pp.476-483.

3. Englar, R. J., et al, "Design of the Circulation Control Wing STOL Demonstrator Aircraft," AIAA Paper 79-1842, August 1979.

4. Englar, R. J. and C. A. Applegate, "Circulation Control - A Bibliography of DTNSRDC Research and Selected Outside References (January 1969 to December 1983)," DTNSRDC-84/052, September 1984.

5. Englar, Robert J., "Application of Pneumatic Lift and Control Surface Technology to Advanced Transport Aircraft," presented at *Transportation Beyond 2000: Engineering Design for the Future*, Conference at NASA Langley Research Center, Hampton, VA, September 26-28, 1995. Published in NASA Conference Proceedings, March 1996.

6. Englar, Robert J., Marilyn J. Smith, Sean M. Kelley and Richard C. Rover III, "Application of Circulation Control Technology to Advanced Subsonic Transport Aircraft, Part II: Transport Application," AIAA Paper No. 93-0644; AIAA *Journal of Aircraft*, Vol. 31, No. 5, Sept-Oct. 1994, pp. 1169-1177.

7. Pugliese, A.J. and R.J. Englar, "Flight Testing the Circulation Control Wing," AIAA Paper 79-1871, August 1979.